NAVAL POSTGRADUATE SCHOOL
Monterey, California

THESIS

SHIP TRACKS
A
GEOGRAPHICAL AND STATISTICAL STUDY

by

John W. Lutz

December, 1992

Thesis Advisor: Philip A. Durkee

Approved for public release; distribution is unlimited.

REPORT DOCUMENTATION PAGE

Form Approved
OMB No. 0704-0188

a REPORT SECURITY CLASSIFICATION UNCLASSIFIED	1b RESTRICTIVE MARKINGS
a SECURITY CLASSIFICATION AUTHORITY	3 DISTRIBUTION/AVAILABILITY OF REPORT Approved for Public Release Distribution Unlimited
b DECLASSIFICATION/DOWNGRADING SCHEDULE	
4 PERFORMING ORGANIZATION REPORT NUMBER(S)	5 MONITORING ORGANIZATION REPORT NUMBER(S)
6a NAME OF PERFORMING ORGANIZATION Naval Postgraduate School	6b OFFICE SYMBOL (If applicable) 35
7a NAME OF MONITORING ORGANIZATION Naval Postgraduate School	
6c ADDRESS (City, State, and ZIP Code) Monterey, CA 93943-5000	7b ADDRESS (City, State, and ZIP Code) Monterey, CA 93943-5000
8a NAME OF FUNDING/SPONSORING ORGANIZATION	8b OFFICE SYMBOL (If applicable)
8c ADDRESS (City, State, and ZIP Code)	10 SOURCE OF FUNDING NUMBERS PROGRAM ELEMENT NO. / PROJECT NO. / TASK NO. / WORK UNIT ACCESSION NO.

TITLE (Include Security Classification)

SHIP TRACKS A GEOGRAPHICAL AND STATISTICAL STUDY

PERSONAL AUTHOR(S)
Lutz, John, W.

13a TYPE OF REPORT	13b TIME COVERED	14 DATE OF REPORT (Year, Month, Day)	15 PAGE COUNT
Master's Thesis	FROM _____ TO _____	December 1992	73

SUPPLEMENTARY NOTATION The views expressed in this thesis are those of the author and do not reflect the official policy or position of the Department of Defense or the U.S. Government.

COSATI CODES			18 SUBJECT TERMS (Continue on reverse if necessary and identify by block number)
FIELD	GROUP	SUB-GROUP	Remote Sensing, Ship Tracks

ABSTRACT (Continue on reverse if necessary and identify by block number)
Anomalous cloud lines are frequently seen in satellite images as curvilinear features. These cloud lines or "ship tracks" are likley due to products of ship-produced hot exhaust gases that are expelled into the atmosphere, increasing the aerosol concentration in the ship track plume. NOAA 9 and 10 AVHRR data are sensitive to cloud droplet size and show the ship tracks as increases in radiance due to reflectance. Twenty eight NOAA 9/10 satellite passes are analyzed. Twenty two of the passes are found to contain a total of 316 ship tracks which is significantly more than that expected by earlier ship track studies. An existing ship track detection algorithm is used to conduct a statistical comparison of ship track and non-ship track, or ambient pixel reflectance of the NOAA 9 and 10 AVHRR channels 1 (0.63 μm), 3 (3.7 μm), and 4 (11 μm). The results of the statistical analysis confirm, as found in previous studies, that the ship track pixels displayed a significant increase in values for channels 1 and 3 and a very slight increase for channel 4.

20 DISTRIBUTION/AVAILABILITY OF ABSTRACT X UNCLASSIFIED/UNLIMITED ☐ SAME AS RPT ☐ DTIC USERS	21 ABSTRACT SECURITY CLASSIFICATION Unclassified
22a NAME OF RESPONSIBLE INDIVIDUAL Philip A. Durkee	22b TELEPHONE (Include Area Code) (408) 656-3465
	22c OFFICE SYMBOL 64/De

Form 1473, JUN 86 Previous editions are obsolete SECURITY CLASSIFICATION OF THIS PAGE
S/N 0102-LF-014-6603 Unclassified

Approved for public release; distribution is unlimited.

SHIP TRACKS
A
GEOGRAPHICAL AND STATISTICAL STUDY

by

John W. Lutz
Lieutenant Commander, United States Navy
B.S., University of Nebraska

Submitted in partial fulfillment
of the requirements for the degree of

MASTER OF SCIENCE IN METEOROLOGY AND PHYSICAL OCEANOGRAPHY

from the

NAVAL POSTGRADUATE SCHOOL
December 1992

Author: _____
John W. Lutz

Approved by: _____
Philip A. Durkee, Thesis Advisor

_____
Carlyle H. Wash, Second Reader

_____
Robert L. Haney, Chairman
Department of Meteorology

ABSTRACT

Anomalous cloud lines are frequently seen in satellite images as curvilinear features. These cloud lines or "ship tracks" are likely due to products of ship-produced hot exhaust gases that are expelled into the atmosphere, increasing the aerosol concentration in the ship track plume. NOAA 9 and 10 AVHRR data are sensitive to cloud droplet size and show the ship tracks as increases in radiance due to reflectance. Twenty eight NOAA 9/10 satellite passes are analyzed. Twenty two of the passes are found to contain a total of 316 ship tracks which is significantly more than that expected by earlier ship track studies. An existing ship track detection algorithm is used to conduct a statistical comparison of ship track and non-ship track, or ambient pixel reflectance of the NOAA 9 and 10 AVHRR channels 1 (0.63 μm), 3 (3.7 μm), and 4 (11 μm). The results of the statistical analysis confirm, as found in previous studies, that the ship track pixels displayed a significant increase in values for channels 1 and 3 and a very slight increase for channel 4.

TABLE OF CONTENTS

I. INTRODUCTION....1
A. BACKGROUND....1
B. AEROSOLS....2
C. CLOUD MICROPHYSICAL PROPERTIES AND RADIATION....3
1. Absorption and Emission....4
2. Scattering....4
3. Reflectance....5
D. SHIP EXHAUST PRODUCED CLOUDS....6
E. OBJECTIVES AND ORGANIZATION....8

II. DATA PROCESSING AND ANALYSIS....9
A. SATELLITE....9
B. SENSOR....9
C. SIGNAL PROCESSING AND CALIBRATION....10
1. Channel 1....11
2. Channel 4....11
3. Channel 3....12
a. Channel 3 Radiance....12
b. Channel 3 Reflectance....12
D. SHIP TRACK GEOGRAPHICAL STUDY....13
E. STATISTICAL STUDY....13

III. RESULTS....26
A. SHIP TRACK FREQUENCY AND GEOGRAPHICAL ANALYSIS....26
B. STATISTICAL STUDY....30

IV. CONCLUSIONS AND RECOMMENDATIONS....59

LIST OF REFERENCES....61

INITIAL DISTRIBUTION LIST....63

LIST OF FIGURES

Fig. 1. Channel 2 overview.....14

Fig. 2. Channel 3 near-infrared subscene.....15

Fig. 3. Channel 1 visible subscene.....16

Fig. 4. Channel 1 ship tracks.....17

Fig. 5. Channel 3 ship tracks.....18

Fig. 6. Channel 3 subscene with 8 by 8 overlay.....21

Fig. 7. Coakley/Morehead algorithm on Fig. 6 subscene.....22

Fig. 8. Fig. 7 subscene reprocessed.....23

Fig. 9. Scatter plot, Chn1 reflectivity vs. Chn3 radiance..24

Fig. 10. Scatter plot, Chn1 reflectivity vs. Chn4 radiance..25

Fig. 11. Channel 1 ship tracks, 1 - 19 July 1987.....27

Fig. 12. Channel 3 ship tracks, 1 - 19 July 1987.....28

Fig. 13. Chn1/Chn3 ship tracks combined, 1 - 19 July 1987...29

Fig. 14. Scatter plot from Table 4 - File number 8.....34

Fig. 15. Scatter plot from Table 4 - File number 9.....35

Fig. 16. Scatter plot from Table 4 - File number 10.....36

Fig. 17. Scatter plot from Table 4 - File number 11.....37

Fig. 18. Scatter plot from Table 4 - File number 12.....38

Fig. 19. Scatter plot from Table 4 - File number 13.....39

Fig. 20. Scatter plot from Table 4 - File number 14.....40

Fig. 21. Scatter plot from Table 4 - File number 15.....41

Fig. 22. Scatter plot from Table 4 - File number 16.....42

Fig. 23. Scatter plot from Table 4 - File number 17.....43
Fig. 24. Scatter plot from Table 4 - File number 18.....44
Fig. 25. Scatter plot from Table 4 - File number 19.....45
Fig. 26. Scatter plot from Table 4 - File number 20.....46
Fig. 27. Scatter plot from Table 4 - File number 21.....47
Fig. 28. Scatter plot from Table 4 - File number 22.....48
Fig. 29. Scatter plot from Table 4 - File number 23.....49
Fig. 30. Scatter plot from Table 4 - File number 24.....50
Fig. 31. Scatter plot from Table 4 - File number 25.....51
Fig. 32. Scatter plot from Table 4 - File number 26.....52
Fig. 33. Scatter plot from Table 4 - File number 27.....53
Fig. 34. Scatter plot from Table 4 - File number 28.....54
Fig. 35. Scatter plot from Table 4 - File number 70.....55

ACKNOWLEDGEMENTS

I would like to thank Dr. Philip A. Durkee for his untiring support and guidance during the extended length of this project, without which this thesis would not have been completed.

I owe a debt of gratitude to the Naval Postgraduate School Meteorology Department for making the final phases of this report as uncomplicated as it was.

I am especially grateful to my wife for her encouragement, her faith that I could complete the task and for her many prayers.

I. INTRODUCTION

A. BACKGROUND

Much attention has been given to anomalous cloud lines seen in visible and near-infrared satellite images. The source of these anomalous cloud lines were first identified by Conover (1969) as exhaust from ships transiting at sea and are often referred to as ship tracks. He showed that the most likely cause of ship track clouds is the increase in the aerosol content produced by ship exhaust. Ship exhaust is a source of aerosols that act as cloud condensation nuclei (CCN) that have the effect of increasing the number of cloud droplets while reducing the droplet size (Coakley et al., 1987).

Advanced Very High Resolution Radiometer (AVHRR) data was used in the Coakley et al. (1987) study with Channel 1 at 0.63 μm, Channel 3 at 3.7 μm, and Channel 4 at 11 μm. Coakley et al. suggested that the effects of aerosols on cloud reflectivity may have a much greater influence on the earth's albedo than that due to the direct scattering and absorption by aerosols alone. They developed an algorithm to detect ship tracks automatically by comparing reflectivities of contaminated clouds to those of similar non-contaminated, or ambient clouds. The Coakley et al. algorithm worked well in

areas of uniform cloud cover, but did not perform well in areas without ship tracks, cloud free areas or regions of transition from one cloud regime to another.

Morehead (1988) evaluated the Coakley et al. algorithm incorporating improvements in its ability to detect ship tracks. The modified algorithm was used in this study to statistically analyze and compare the radiative properties of the ship tracks found in data gathered from 1 to 19 July 1987 in the North Pacific Ocean Basin. Three hundred and sixteen ship tracks were observed in this study. The Morehead modified algorithm failed to identify all the ship tracks that were found by visual inspection. It also had a further draw back of identifying non-ship track segments as ship tracks. A manual filtering technique was developed for this thesis to ensure that the statistical analysis was conducted only on confirmed ship track segments. This process will be described in detail in Chapter II. An additional focus of this study was to identify and plot the geographical location of the observed ship tracks. This process will be explained in Chapter III.

B. AEROSOLS

Aerosols alter the atmosphere's ability to scatter and absorb solar radiation. They also affect the radiation budget through their effect on clouds. The ability of aerosols to effect clouds comes from their function as CCN which serve as anchors on which cloud droplets can form. Atmospheric

particle size distributions cover a large range. CCN have a radius of about 0.1 μm, cloud droplets have an average radius of 10 μm, and large cloud droplets have a radius of 100's of μm. While CCN are too small on their own to have a significant interaction with incoming solar radiation, once cloud droplets form around them their interaction with incoming solar radiation is very much greater.

Ships are a source of aerosols in the atmosphere. Exhaust expelled onto the atmosphere is in the form of water vapor, gaseous constituents and aerosols. Aerosols are of the size to act as CCN, as discussed above, and boost the CCN concentration far above the normal level. Twomey (1968, 1984) and Hindman et al. (1977) have described how the concentration and size distribution of CCN have a direct impact on the formation of cloud droplets. The new source of CCN from ship exhaust will cause a change in reflective properties of clouds. Twomey and Cocks (1982) show that an increase in droplet concentration causes a decrease in the size of the droplet. The shift in droplet size, along with an increase in concentration, will result in a significant increase in reflectance due to scattering.

C. CLOUD MICROPHYSICAL PROPERTIES AND RADIATION

Electromagnetic energy reacts with the atmosphere either by scattering or absorption. Energy that is absorbed is converted to an increase in the temperature of the absorbing body. The atmosphere, having a temperature, can also emit

electromagnetic energy. These processes represent the interactions that take place in the atmosphere. The source of radiation reaching a satellite is then due to either reflection or emission. Reflection results from energy entering the atmosphere and undergoing single or multiple scattering events until it is directed back out the top of the atmosphere, primarily affecting short wave solar radiation. Energy which is absorbed is converted into an increase in temperature of the absorbing body which can subsequently undergo emission at a multitude of wavelengths including long wave frequencies.

1. Absorption and Emission

The atmosphere has a direct impact on satellite measured radiance due to absorption and emission. Clouds are composed primarily of liquid water, so absorptive properties of water are a primary concern. Liquid water absorbs electromagnetic energy at all wavelengths. The absorption is much greater at the infrared wavelengths than in the visible. This leads to greater emission at the longer infrared wavelengths.

2. Scattering

The type of scattering interactions depend on the cross-sectional area of the particle with which the energy is interacting. When the scattering particle size and the wavelength of the incident energy are of the same order, the interaction is best described by the Mie scattering theory.

For the particles in this category, the scattering properties become less dependent on the wavelength and more dependent on particle size. Mie scattering has a greater percentage of scatter in the forward direction than to the side or backward direction. As the droplet radius increases, forward scattering increases and backward scattering decreases.

3. Reflectance

In this study we are considering reflectance, the measure of energy reflected, from cloud surfaces. At the wavelengths considered, the reflectance depends most heavily on Mie scattering processes. A useful measure of the degree of scattering can be found by examining the optical depth of the cloud layer. Twomey (1977) concluded that pollution (or ship stack exhaust in the case of this study), by increasing cloud nucleus concentration, hence increasing the numbers of cloud droplets; leads to increased cloud optical depth which increases cloud reflectivity. Hunt (1972) described the phase scattering characteristics as well as the particle size effects on reflectance of cloud layers in the visible and infrared windows. He showed that the changes in cloud radiative properties at the visible and infrared wavelengths are consistent with changes in the size distribution of particles such that, as the radius of the cloud droplets decreases the reflectance increases.

D. SHIP EXHAUST PRODUCED CLOUDS

Ship tracks appear as curvilinear features at visible and near-infrared wavelengths in satellite imagery. They have a plume like nature, narrow at the source and spreading horizontally with distance from the source. Ship tracks can be several hundred kilometers in length and can last for days.

It appears that there are two different types of ship tracks. The first are seen in the visible satellite imagery where anomalous cloud lines form in areas where cloud formation is suppressed. These may be produced as the ship enters an area where the atmosphere is experiencing a CCN deficit. As the CCN from the exhaust gases mix with the air, the deficit is reduced enough for clouds to form. Another theory is that the cloud free region is in an area where the cloud droplets are of sufficient size to precipitate out therefore keeping the area free of clouds. As the ship passes through the area, the addition of the exhaust gas CCN reduces the size of the droplets so that they are no longer large enough to precipitate out and thus the cloud forms (Albrecht, 1990).

The second type of ship track can be seen in the near-infrared (NIR) satellite imagery. These are generated in cloudy areas and are detectable in the NIR due to the shift to smaller size cloud droplet distribution from the addition of CCN. These are not seen in the visible because at 0.63 μm there is no absorption. Therefore, the reflectance becomes

primarily a function of the liquid water property and size distribution. At 3.7 μm, there is moderate absorption hence reflectance becomes primarily dependent on the particle radius. At 11 μm, there is high absorption and the particle acts as a black body with no reflectance.

Fett et al. (1979) indicated that the most common areas of ship track formation were in regions of closed cellular clouds with medium base heights. Morehead (1988) pointed out that other conditions which help to promote ship track formation include areas with saturated or supersaturated air near the top of the marine layer; areas where the air temperature is cooler than the sea-surface temperature; or areas where there is a minimum of vertical wind shear. Saturated air at the top of the boundary layer provides sufficient moisture to form cloud droplets in the presence of the increase of CCN provided by the ship exhaust. The warm sea surface temperature enhances track formation in the presence of a moist boundary layer by creating an environment which is more favorable to fog and haze. The effect of wind shear in the boundary layer would be to disperse the CCN provided by the exhaust resulting in poorly defined or nonexistent cloud lines. Ship track cloud formation will be further enhanced in areas of stratus/stratocumulus cloud topped boundary layers, eastern oceans, and high latitudes.

E. OBJECTIVES AND ORGANIZATION

The goal of this thesis is to analyze ship track data over an extensive data base of AVHRR satellite imagery using the ship track detection algorithm developed by Coakley et al. (1987) and modified by Morehead (1988). This study will have two basic objectives. One is to develop a summary of where geographically the ship tracks most often occurred during the study period. An additional focus is to conduct a statistical evaluation of confirmed ship tracks to compare the relationship and contrasts between AVHRR channel 1 reflectivity and AVHRR channels 3 and 4 radiance for ship track areas versus non-ship track areas.

Chapter II will discuss the data used in the study as well as the satellite and sensor used to obtain the data. Chapter II will discuss the analysis used in the two parts of this study, including the techniques used to manipulate the data for determining ship track geographical locations and the techniques used in the statistical study. The results of the analysis will be presented in Chapter III and Chapter IV will contain the conclusions which are drawn from the results and recommendations for future work.

II. DATA PROCESSING AND ANALYSIS

The first part of Chapter II describes the satellite platform and sensor used to collect the data for this study. Then, the source and format of the data will be discussed as will the basic signal processing and calibration which is conducted prior to use by the ship track cloud retrieval algorithm.

A. SATELLITE

The platforms providing the data for this study were the NOAA 9 and 10 polar orbiting satellite series sponsored by the National Oceanic and Atmospheric Administration (NOAA). The satellites fly sun-synchronous polar orbits at an altitude of about 525 nautical miles. The NOAA 9/10 series provided coverage for different times of the day. NOAA-9 satellite passes were generally around 2300 UTC (1500 local standard time) and are roughly parallel to the North American coast. NOAA-10 passes were at 1600 UTC (0800 local standard time) and cut NE-SW across the central California coast. The data were collected by Scripps Satellite Oceanography facility in La Jolla, California.

B. SENSOR

Radiance data on the NOAA 9/10 satellites are collected by the Advanced Very High Resolution Radiometer (AVHRR)

instrument. This sensor provided a nadir resolution of 1km by 1km at the polar orbit altitude of 525 N mi.

Table 1 shows the five wave bands recorded by the AVHRR sensor. Channel 1 is in the visible, channels 2 and 3 are in

TABLE 1
WAVEBANDS OF THE ADVANCED
VERY HIGH RESOLUTION RADIOMETER (AVHRR)

Channel	Wavebands (μm)	Center Frequency (μm)
1	0.58 - 0.68	0.63
2	0.73 - 1.10	0.83
3	3.55 - 3.93	3.7
4	10.30 - 11.30	11.0
5	11.50 - 12.50	12.0

the near-infrared, and channels 4 and 5 are in the thermal infrared portion of the electromagnetic spectrum.

Channel 2 was used to prepare the satellite pass overview that distinguished what areas to investigate for possible ship tracks. Channels 1, 3 and 4 were used in the ship track detection algorithm.

C. SIGNAL PROCESSING AND CALIBRATION

The development of cloud analysis algorithms as part of the International Satellite Cloud Climatology Project (ISCCP) motivated the collection of the data used in this study. All the data were part of the First ISCCP Regional Experiment

(FIRE) conducted in the summer of 1987. All the high density tapes used for the analysis had been previously navigated for the FIRE study.

The original data came on high density tapes in the form of counts of radiant energy in each of the five channels listed above. The radiant energy data were calibrated and converted to geophysical parameters. The calibration of channels 1, 3 and 4 is discussed briefly below and is discussed in full by Allen (1987).

1. Channel 1

This is the visible channel, which was used in this study to search for areas where the potential for finding ship tracks was greatest. Since it is known that ship tracks are not likely to be found in cloud free regions in the visible, these areas could be avoided. The calibration of channel 1 data is accomplished assuming a linear relationship between counts received by the sensor and the reflectance. The calibration is done in terms of albedo and the results are in units of percent of reflectance.

2. Channel 4

Channel 4 imagery is used to help classify cloud masses. It is used in the Coakley algorithm to help locate non-ship track pixels with similar microphysical properties as nearby ship track pixels. Channel 4 data result mainly from

thermal emission. The data are converted to radiance measurements with units of W/m^2-sr-cm^{-1} using a linear correlation to counts of radiant energy.

3. Channel 3

The channel 3 near-infrared band data contains the most important information for ship track detection. Ship tracks show up very clearly in channel 3 while they may not be detected in other wavelengths. Channel 3 data is comprised of both reflectance and thermal emittance information for daylight passes. As discussed by Morehead (1988), two types of channel 3 data are used:

a. Channel 3 Radiance

The first is a channel 3 radiance which contains both the reflectance and emission contributions, determined by a linear correlation between counts measured and radiance, with units of W/m^2-sr-cm^{-1}.

b. Channel 3 Reflectance

The second is a channel 3 reflectance signature estimating only that portion of the measured irradiance resulting from reflectance.

The reflectance is derived from the channel 3 radiance and the channel 4 radiance which represents the thermal emission. The channel 4 data are used to estimate emission in channel 3. This emission is subtracted from the total radiance leaving only a reflectance.

D. SHIP TRACK GEOGRAPHICAL STUDY

One focus of this analysis was to determine geographically where the ship tracks formed during the period of the study (1 - 19 July, 1987). Each AVHRR data tape processed contained an overview image consisting of one satellite pass of the North Pacific Ocean basin (Figure 1). Each pass was subjectively scanned, subscene by subscene (500km by 500km), in both channel 3 and channel 1 to locate ship track clouds (Figures 2 and 3). Once a ship track was found, latitude and longitude positions were traced along the ship track. The ship tracks were then plotted to show their location. Geographical diagrams were produced for each pass showing the position and track of all ship tracks found in both channel 1 and channel 3. Figure 4 and Figure 5 show the geographical plots of ship tracks found in channel 1 and channel 3 respectively, for the 7 July pass whose overview is shown in Figure 1.

E. STATISTICAL STUDY

The second part of this study involved a statistical comparison of channels 1, 3 and 4. An algorithm developed by Coakley et al. (1987) and modified by Morehead (1988) was applied to each subscene determined to contain ship tracks,as found in the geographical process above. The result of each subscene statistical analysis was compared to the respective

Figure 1. Channel 2 overview: NOAA-9 satellite pass AR6085 (2237 UTC, 7 July 1987). Displays the location of the subscene used as an example of the data processing of this thesis.

Figure 2. Channel 3 near-infrared subscene: AR6085 (2237 UTC, 7 July 1987).

Figure 3. Channel 1 visible subscene: AR6085 (2237 UTC, 7 July 1987).

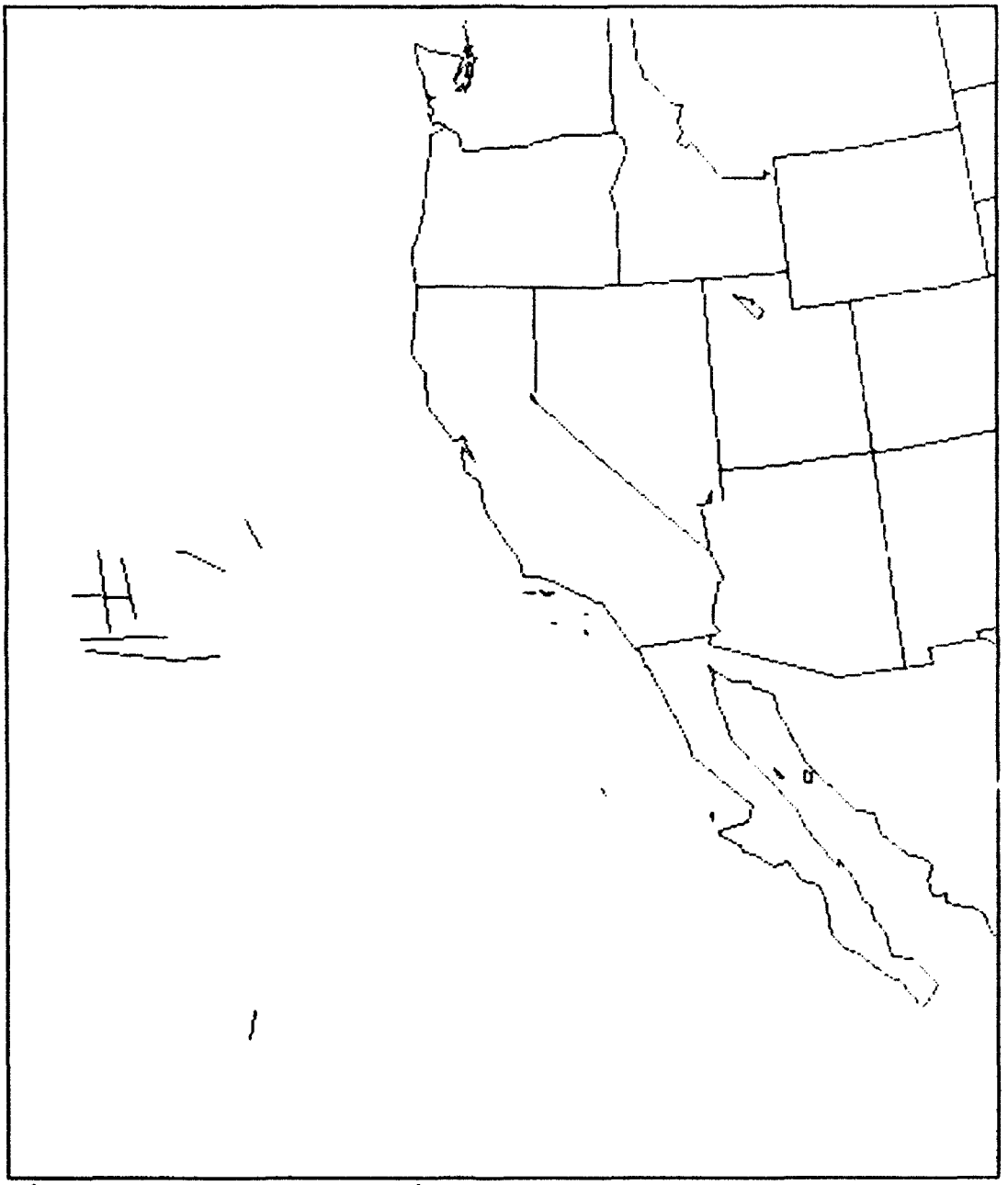

Figure 4. Channel 1 ship tracks: AR6085 (2237 UTC, 7 July 1987).

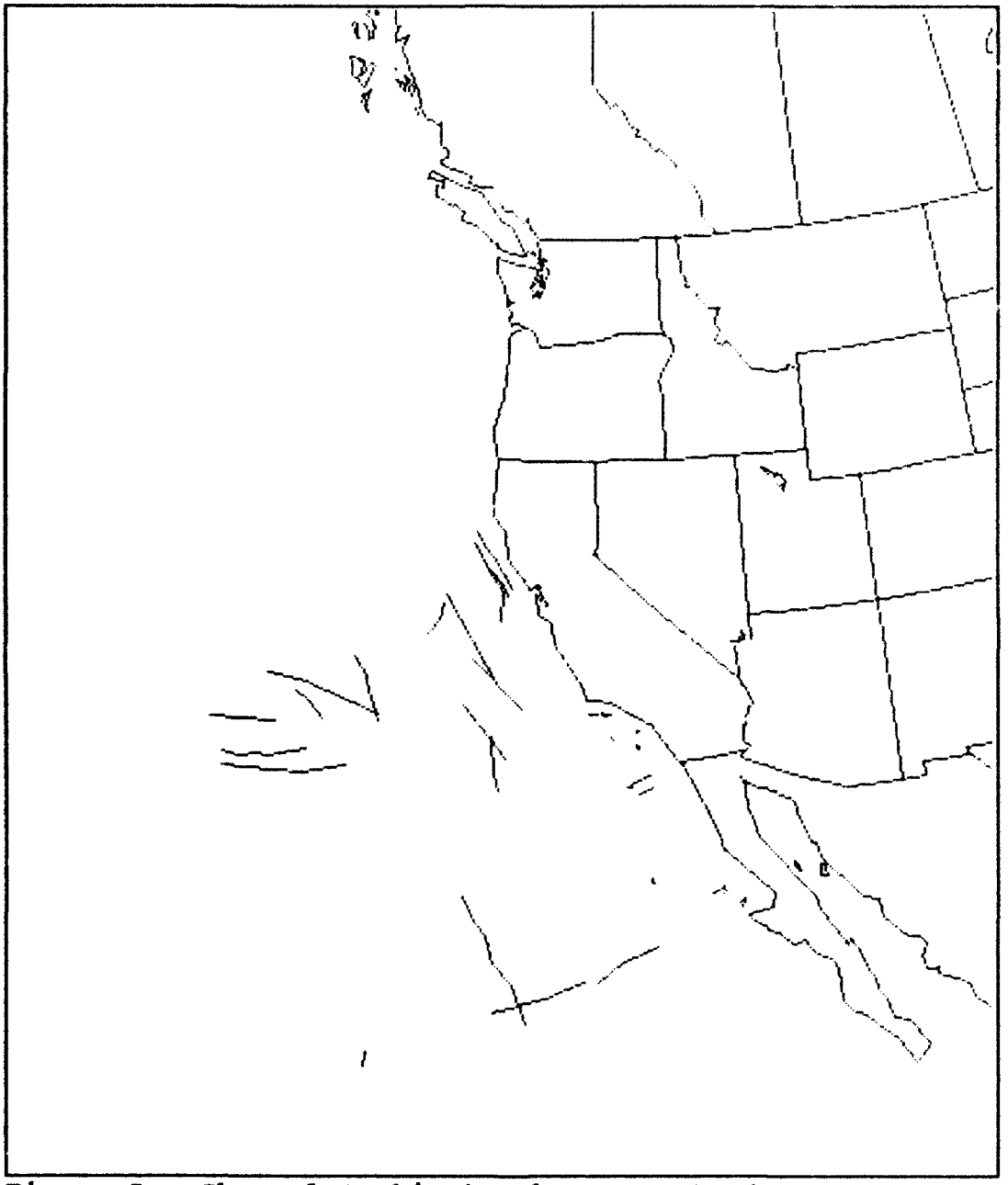

Figure 5. Channel 3 ship tracks: AR6085 (2237 UTC, 7 July 1987).

channel 3 image. A numbered 8 by 8 grid of 64 pixel squares was overlaid on both the statistical image and the channel 3 image. The numbered squares (1 - 64) facilitated in selecting which pixel areas to filter out. Only the grid areas with confirmed ship track data were reprocessed, filtering out non-ship track statistical data.

This process is shown for the NOAA-9 pass on 7 July 1987, in Figures 6, 7 and 8. Figure 6 shows a channel 3 subscene with ship tracks clearly visible as dark curvilinear lines with an 8 by 8 grid overlaid. Figure 7 shows the results of the Coakley/Morehead algorithm processed on the subscene. Figure 8 shows the reprocessed analysis with the non-ship track lines filtered out and the normal or ambient control points included. The filtering process was conducted to create a statistical data base representing as near as possible, only confirmed ship tracks. The final step in the analysis was to process grid points containing confirmed ship tracks through a comparison routine of ship track vs. ambient pixels, giving values of reflectance for channel 1 and radiance for channels 3 and 4. The results of this routine were presented in tabular and scatter plot format with comparisons among channels 1, 3 and 4. Figures 9 and 10 are the scatter plots for the case presented in Figures 6 through 8 above. Figure 9 shows the comparison of channel 1 reflectivity to channel 3 radiance. Ambient pixels are represented by (·)s and enclosed by a solid ellipse.

Ship track pixels are represented by (+)s and enclosed by a dashed ellipse. The increase in reflectivity in channel 1 and radiance for channel 3 for the ship track pixels can be readily seen in Figure 9. Figure 10 shows a comparison between channel 1 reflectivity and channel 4 radiance. It is noted that there is very little difference between the ambient and ship track pixel values in this comparison. This result will be discussed further in Chapter III.

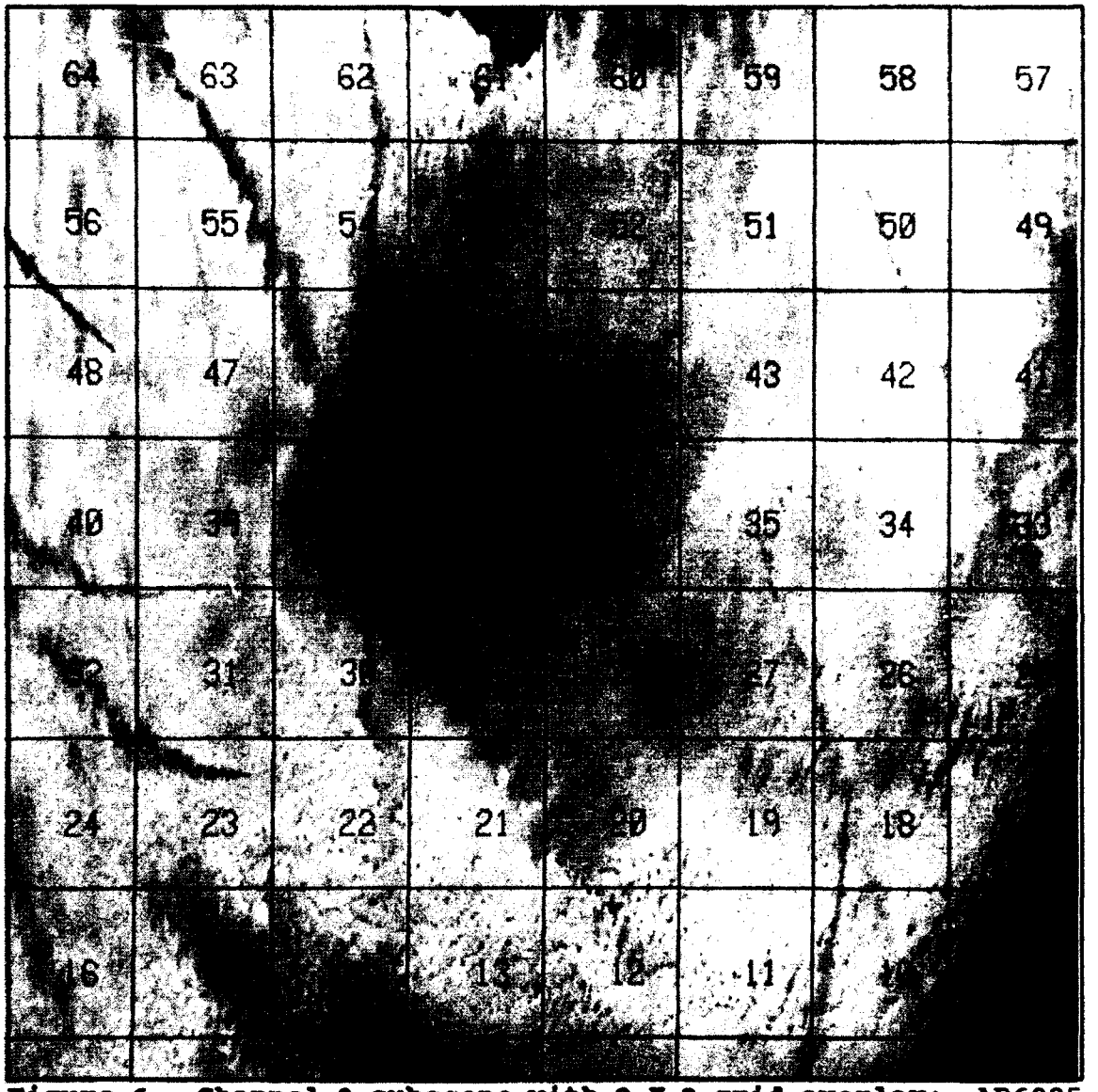

Figure 6. Channel 3 subscene with 8 X 8 grid overlay: AR6085 (2237 UTC, 7 July 1987).

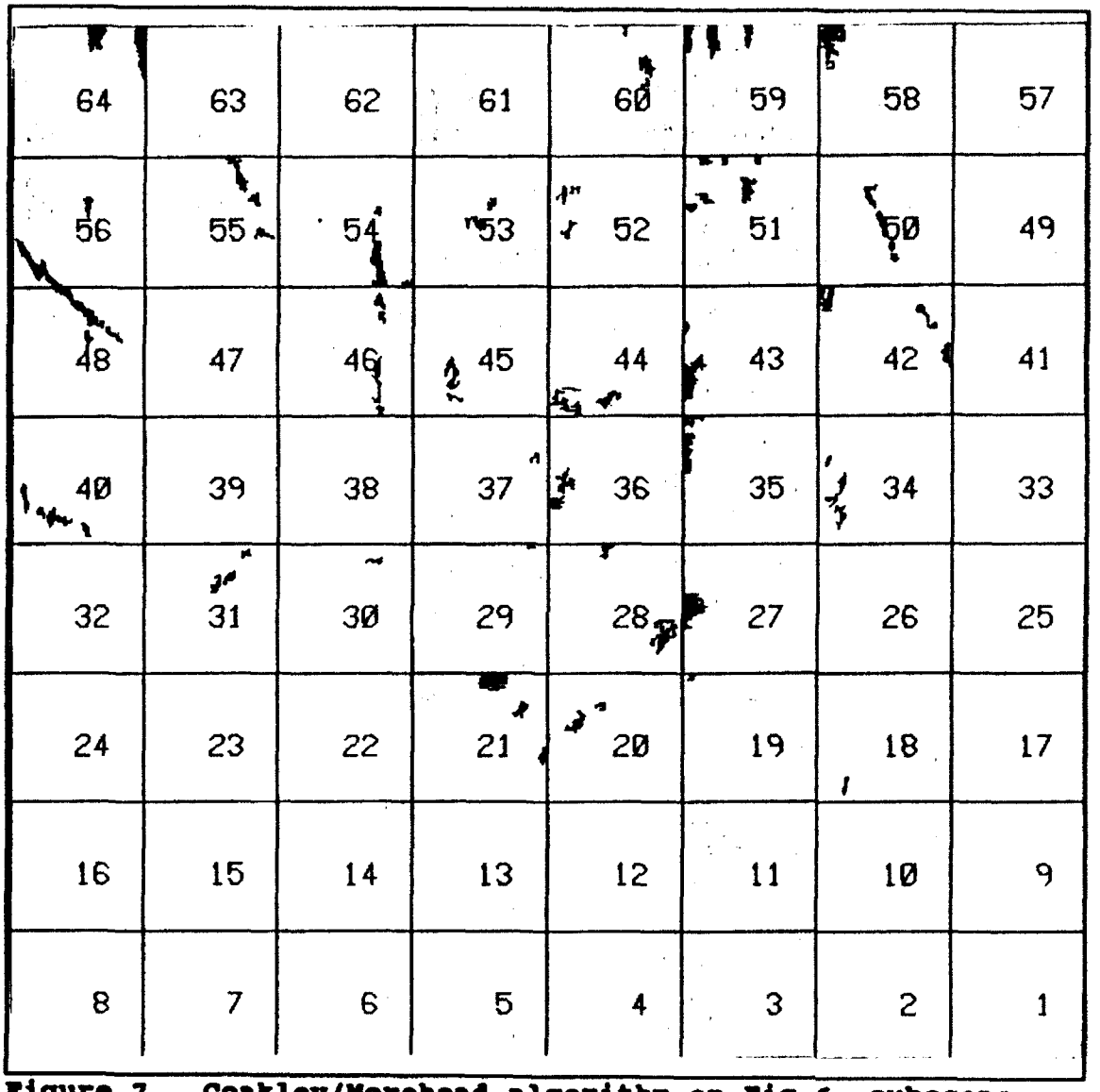

Figure 7. Coakley/Morehead algorithm on Fig 6. subscene.

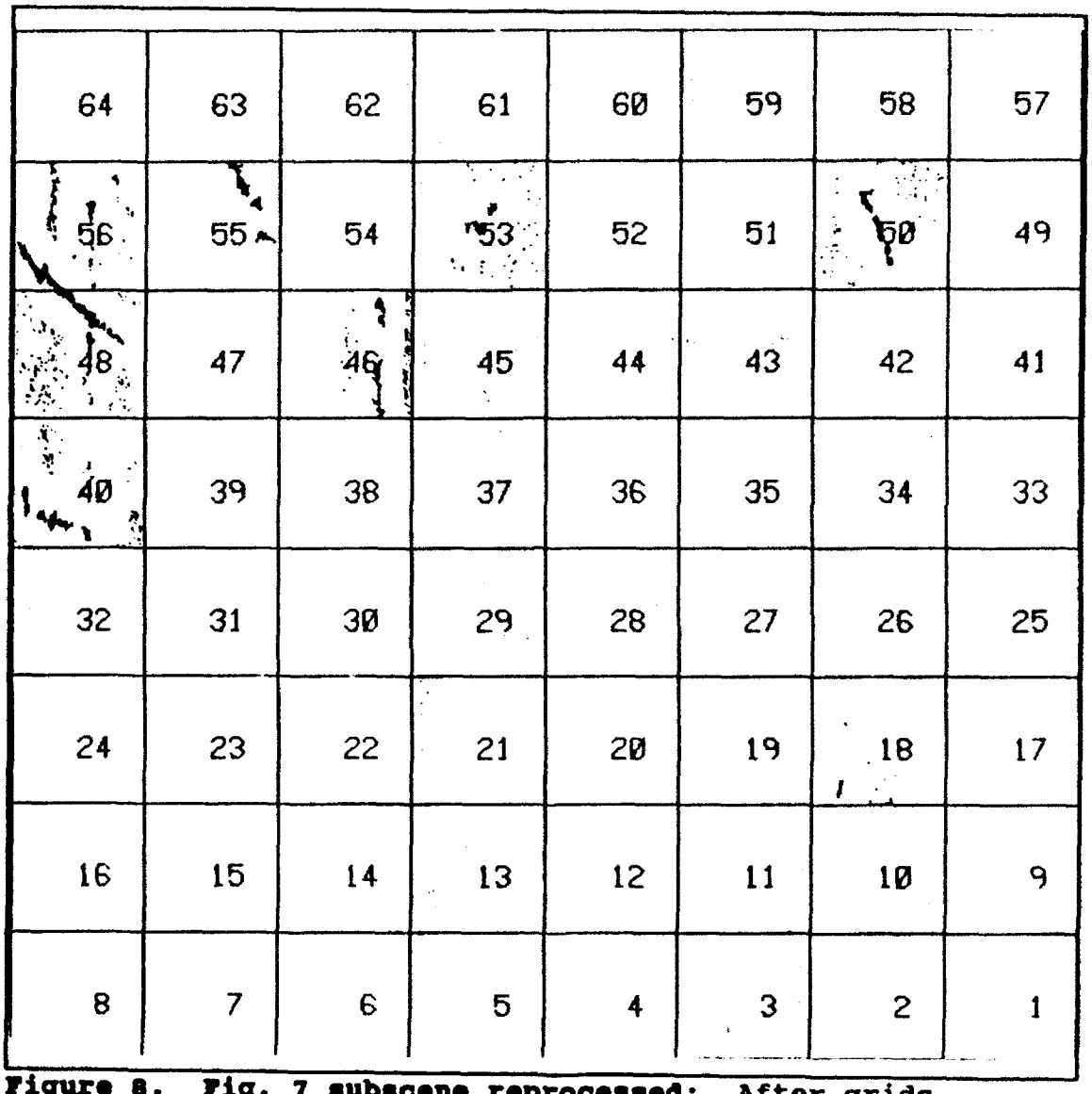

Figure 8. Fig. 7 subscene reprocessed: After grids containing non-ship track analysis were filtered out.

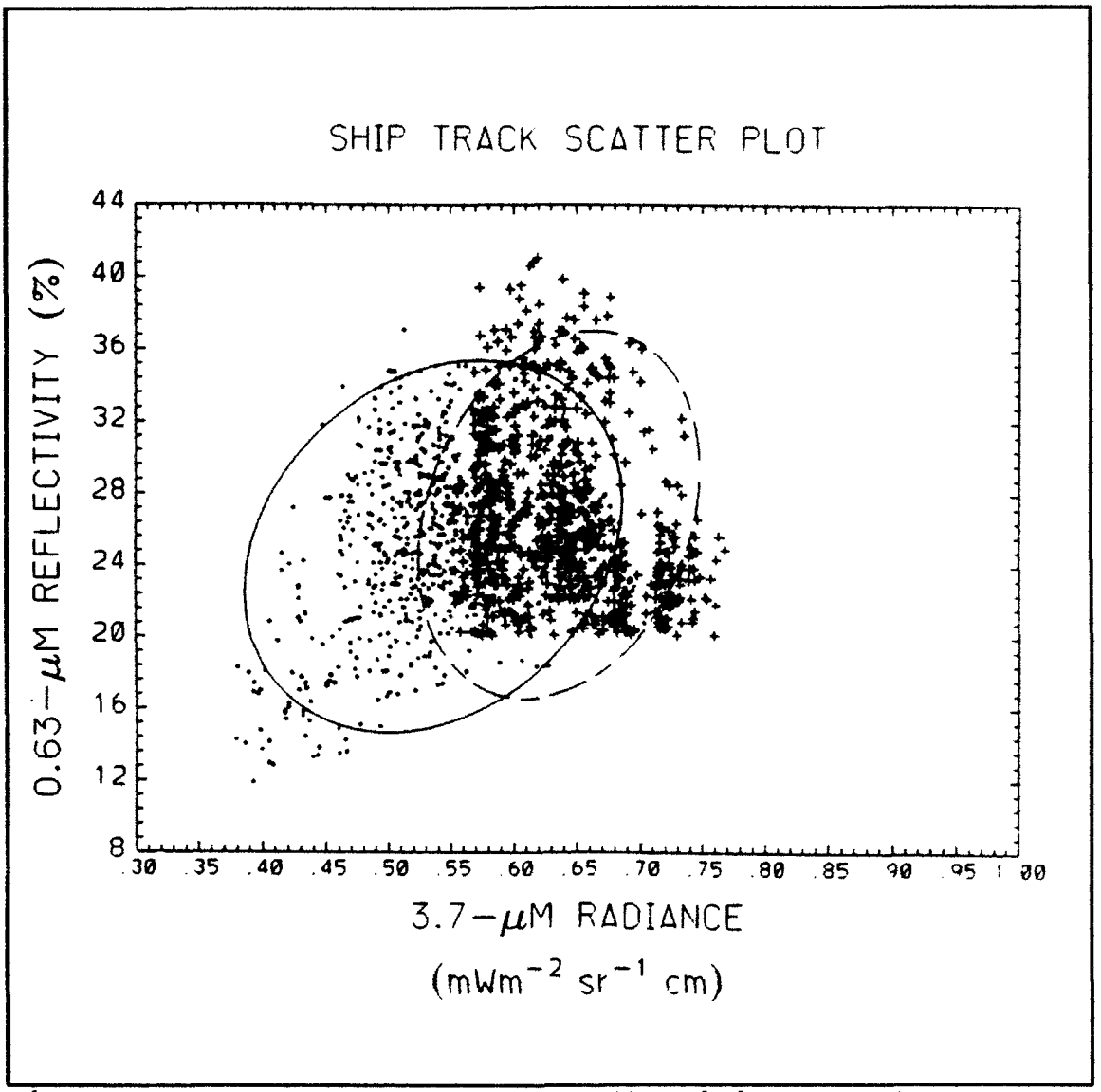

Figure 9. Scatter plot, Chn 1 reflectivity vs. Chn 3 radiance: Ship track pixels (+) and ambient pixels (·).

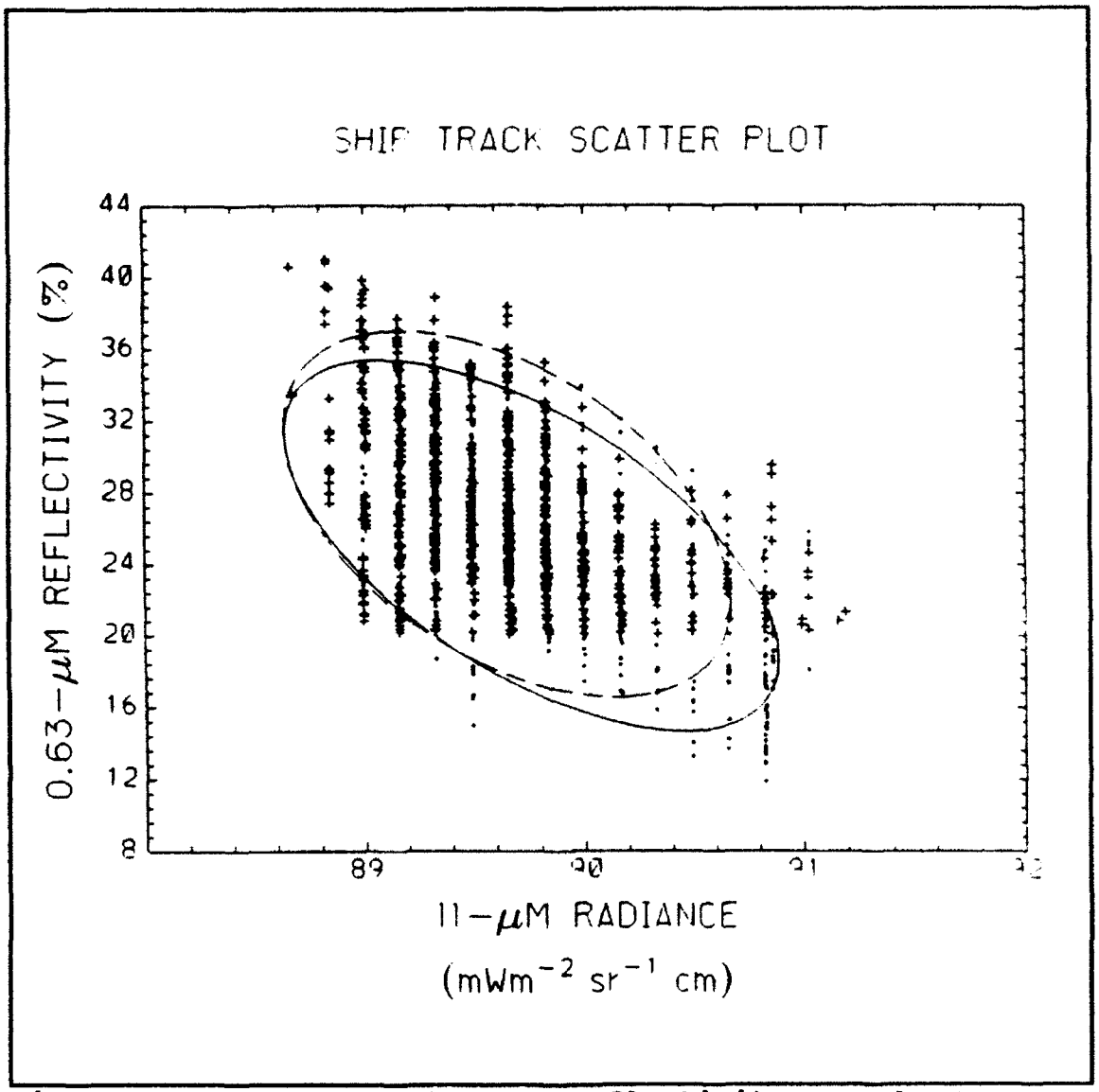

Figure 10. Scatter plot Chn 1 reflectivity vs. Chn 4 radiance: Ship track pixels (+) and ambient pixels (·).

III. RESULTS

A. SHIP TRACK FREQUENCY AND GEOGRAPHICAL ANALYSIS

Coakley et al. (1987) made an assessment that ship tracks would occur in only 5 to 10% of all orbital passes. During the course of this study, 28 NOAA passes (17 NOAA - 9, 11 NOAA - 10) were analyzed. This encompassed 17 days from 1 to 19 July 1987. During this period, 408 subscenes (500km by 500km) were examined leading to the discovery of 316 ship tracks. Table 2 provides a summary of the ship tracks found

TABLE 2
RESULTS OF GEOGRAPHICAL ANALYSIS

		PASSES WITH SHIP TRACKS		
SATELLITE	PASSES	IN CHN 3 ONLY	IN CHNs 1 & 3	TOTAL
NOAA-9	17	3	10	13 (76%)
NOAA-10	11	5	4	9 (82%)
TOTAL	28	8 (29%)	14 (50%)	22 (79%)

in the analysis. Only six of the passes did not contain ship tracks in either channel 1 or 3. This analysis found that 79% of all passes studied contained ship tracks, which is

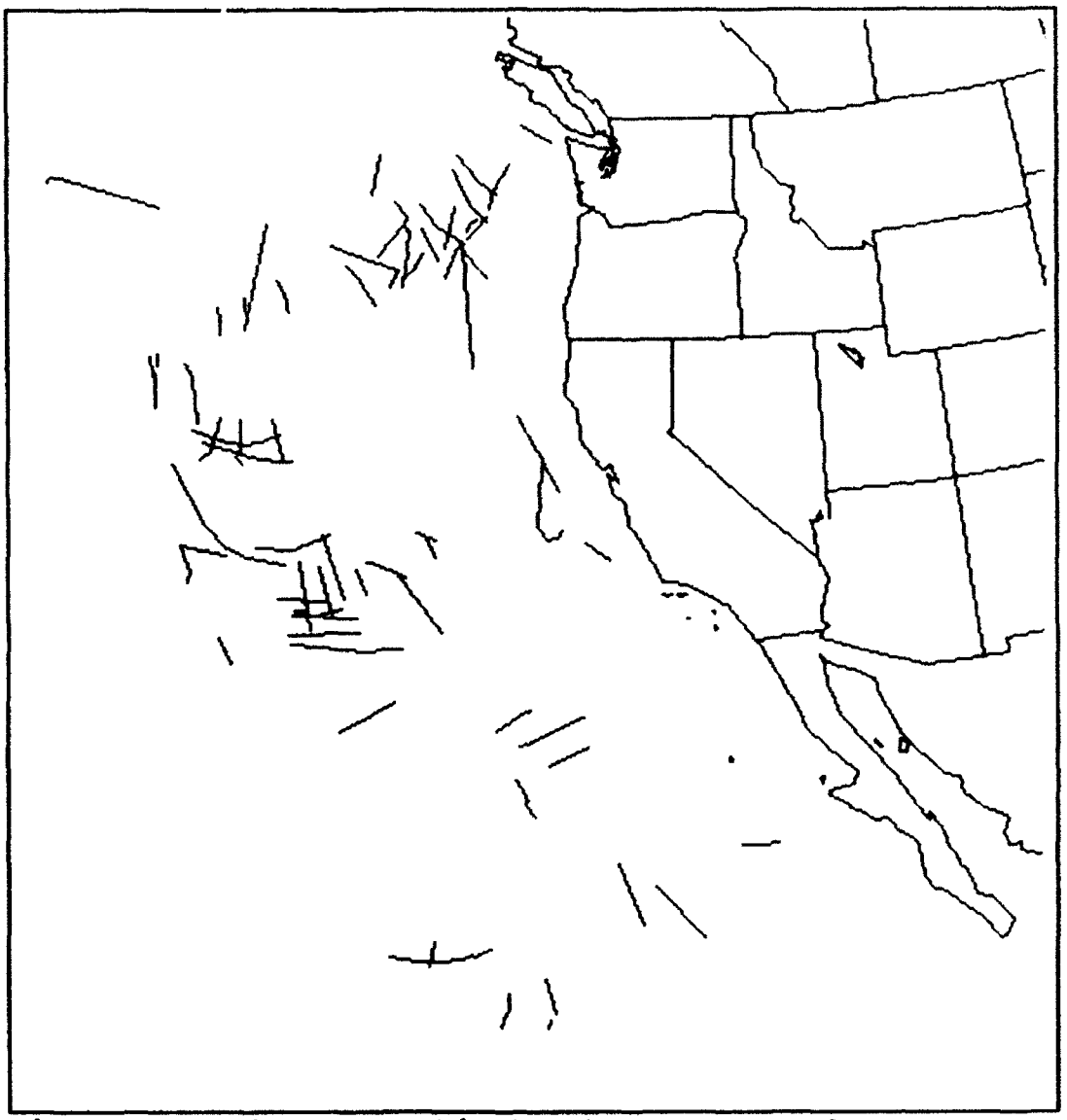

Figure 11. Channel 1 ship tracks, 1 - 19 July 1987.

dramatically higher than the Coakley et al. assessment. Figures 11, 12 and 13 display the plots of ship tracks found in channel 1, 3 and combined respectively for all the passes processed for this study.

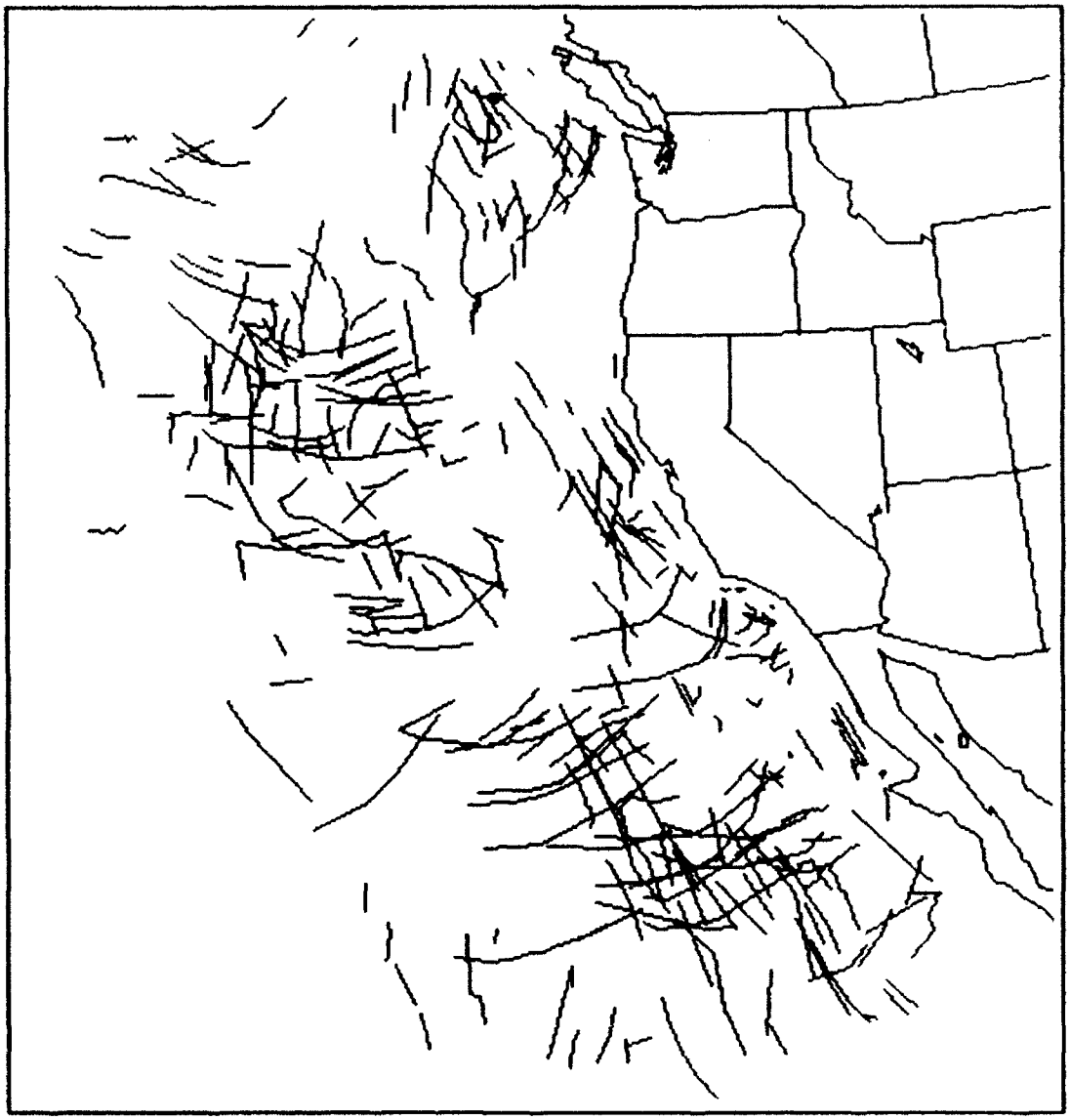

Figure 12. Channel 3 ship tracks, 1 - 19 July 1987.

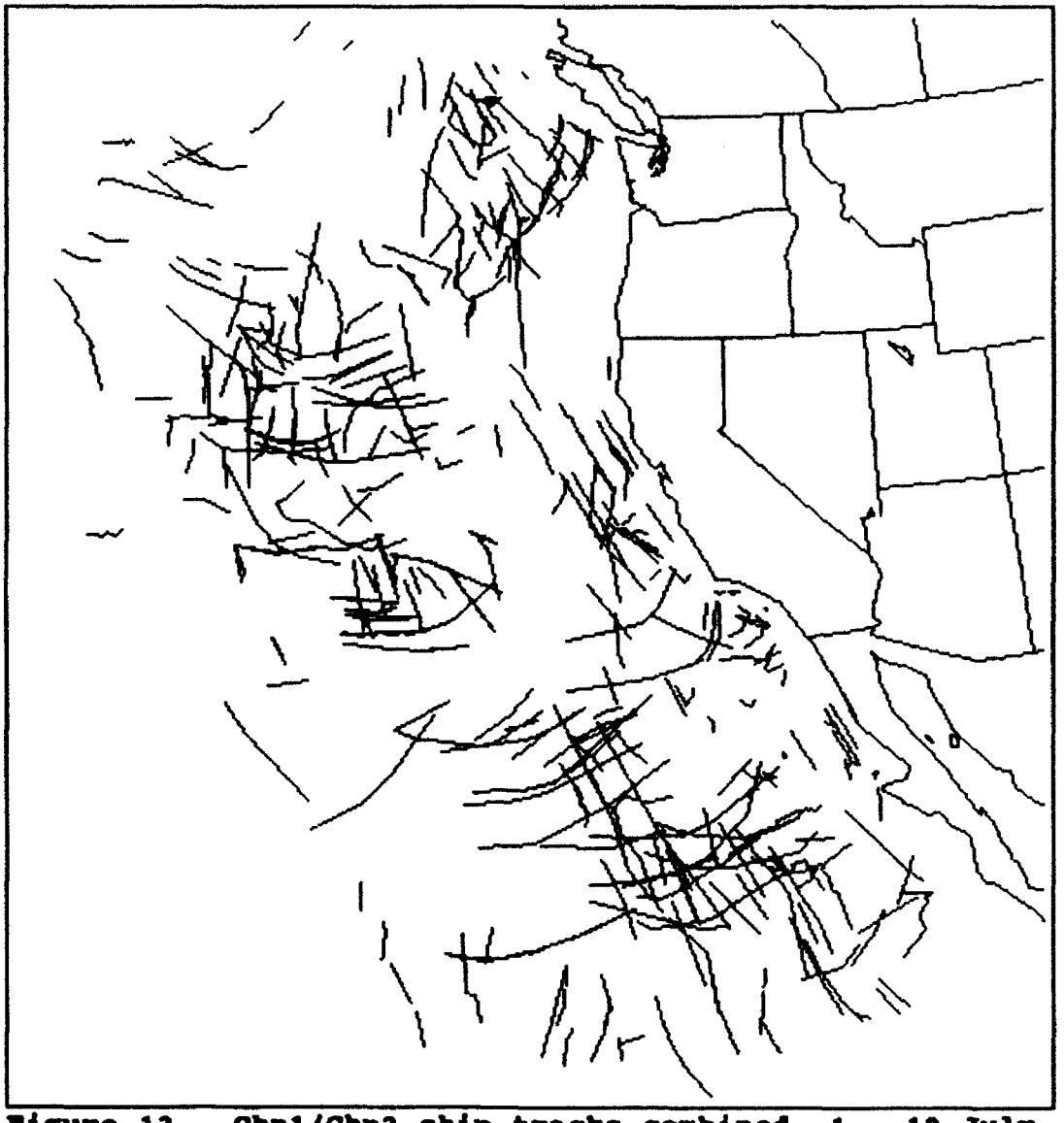

Figure 13. Chn1/Chn3 ship tracks combined, 1 - 19 July 1987.

B. STATISTICAL STUDY

Ship track studies by Coakley et al. (1987) and Morehead (1988) were conducted on special cases with only a limited data set and provided a snapshot of the radiative properties of a few ship tracks. The analysis of this thesis was conducted over a much broader data base. As the geographical analysis was being conducted, all subscenes found to contain ship tracks were annotated for further analysis using the modified Coakley algorithm. Once the filtering process, discussed previously, was completed, a statistical data base was created that provided a data enriched view of the radiative properties of the ship tracks detected.

One of the results from the algorithm was the degree of variability in the radiative and reflective properties of the ship tracks. Table 3 presents the maximum and minimum values of channel 1 reflectivity and channels 3 and 4 radiance for

TABLE 3

	AMBIENT PIXELS MAX	AMBIENT PIXELS MIN	SHIP TRACK PIXELS MAX	SHIP TRACK PIXELS MIN
CHANNEL 1	39.5942	16.9879	45.1522	21.2278
CHANNEL 3	0.9252	0.4462	1.0548	0.5400
CHANNEL 4	96.6457	76.6413	96.6786	76.6425

the ambient and ship track pixels processed. Table 4 gives mean radiance values for the channel 1, 3 and 4 ambient and ship track pixels, for the 61 subscenes processed. When the maximum and minimum values shown in Table 3 are compared to the average of the means from Table 4, one can see that for the ship track pixels, the spread from the average is greater than the spread from the average for the ambient pixels. This implies that the response of clouds to ship effects is not confined to one resulting reflectance value.

Figures 14 through 35 represent some selected scatter plots from the data set. The diagrams plot distributions of channel 1 reflectivity as a function of channel 3 or channel 4 radiance. Pixels contaminated by ship-stack exhaust are designated by (+) and those of randomly selected, nearby ambient fields of view, are designated by (·). The solid (ambient control group) and dashed (ship track) ellipses represent fits at 2 standard deviations to the reflectivity and radiance distributions, which are taken to be joint Gaussian distributions.

The study by Coakley et al. (1987) displayed a similar scatter plot depicting an overall increase in both channel 1 reflectivity and channel 3 radiance for the selected subscene of that study. It can be seen in Figures 14 through 35 that the visible reflectance is not always increased for the ship track group. In fact, only 36 of the 61 files presented in Table 4, had increases in channel 1 reflectivity. Figures 15,

TABLE 4

FILE	AMBIENT PIXEL MEANS			SHIP TRACK PIXEL MEANS		
	CHN 1	CHN 3	CHN 4	CHN1	CHN3	CHN4
8	24.2212	0.5746	88.1291	26.8427	0.7312	88.0581
9	30.5255	0.6044	85.7383	26.4225	0.7269	85.8990
10	21.5716	0.6344	81.7598	24.8219	0.8223	81.9286
11	23.6894	0.4869	87.0027	26.5680	0.6166	86.9501
12	19.6578	0.5098	87.2836	23.5276	0.7178	87.1150
13	21.7656	0.5448	94.4822	21.9398	0.5217	94.5021
14	29.3396	0.6294	90.3357	29.6450	0.6583	90.2409
15	31.9597	0.7016	93.6320	29.8517	0.8053	93.9213
16	27.0591	0.5718	95.3290	24.3910	0.6966	95.3022
17	29.3522	0.7908	76.6858	26.1794	0.9035	77.1182
18	26.3170	0.5304	84.0759	25.3175	0.6337	83.8005
19	22.9589	0.5492	83.8701	21.8956	0.6441	83.9045
20	23.2272	0.4897	79.5234	25.0110	0.6725	79.6512
21	36.1581	0.7652	88.7463	31.4146	0.9425	89.0014
22	19.2665	0.6036	92.6390	23.5893	0.7148	92.6119
23	29.0891	0.6682	96.1202	31.5608	0.7642	96.1592
24	21.5051	0.6262	89.7254	22.8663	0.7222	89.7311
25	28.1713	0.5070	84.7472	33.7518	0.6762	84.4100
26	21.1113	0.8758	91.2801	24.0496	1.0548	91.2875
27	24.8355	0.6130	87.4729	25.1068	0.8872	87.4133
28	22.8464	0.6606	91.0871	22.7940	0.7199	91.1117
29	39.5942	0.4478	76.6411	45.1522	0.5439	76.6425
30	28.8177	0.5888	91.3460	24.5376	0.6909	91.3651
31	27.0589	0.5698	92.3638	24.9227	0.6588	92.3126
32	28.1676	0.7165	89.9115	24.0831	0.8178	89.9542
33	26.6422	0.7545	89.8810	24.8098	0.9758	89.9690
34	24.0577	0.6219	88.4541	24.0284	0.7276	88.4226
35	25.0297	0.6307	88.5494	24.8636	0.7120	88.5269
37	24.7390	0.5837	89.0059	24.3843	0.6614	89.2105
39	35.1769	0.5923	87.6789	37.8106	0.7011	87.6577
40	25.1438	0.6659	90.7080	25.3029	0.7738	90.6777
41	29.1673	0.7102	89.7245	30.4818	0.9291	89.8166
42	22.7745	0.4657	89.3695	24.3685	0.5566	89.3836
43	23.4680	0.4691	91.5017	23.5980	0.5400	91.4679
44	27.1801	0.5121	90.1823	27.4102	0.6162	90.1787
45	26.2157	0.5322	90.8941	26.5164	0.6514	90.9470
46	34.4570	0.8593	92.1994	31.6299	0.9382	92.2850
47	24.0243	0.5657	90.3432	23.3204	0.6870	90.0676
48	24.5518	0.4784	93.6367	24.9595	0.5509	93.6156
49	24.1023	0.4718	93.0157	25.7959	0.5586	92.9459
50	35.5717	0.9252	91.7841	33.4080	1.0335	91.8800
51	31.5178	0.6119	89.8064	28.8882	0.7431	89.7435
52	30.5942	0.6771	90.6243	27.0456	0.7875	90.5918
53	24.9719	0.4900	85.4401	25.4169	0.5748	85.3360
54	27.6829	0.5287	89.7008	28.0631	0.5877	89.7974
55	22.8279	0.5671	92.2144	23.3072	0.6705	92.2388
56	23.7372	0.7285	95.9731	24.1964	0.8741	96.0323
57	21.4856	0.5601	92.8761	21.7729	0.6171	92.8552
58	19.6357	0.4784	89.8637	21.2278	0.6342	89.8880
59	29.0571	0.4462	87.6969	22.8780	0.5470	87.6742
60	23.0665	0.4985	85.9742	27.2078	0.6433	85.8956
61	33.3143	0.4718	80.4961	36.7697	0.6708	80.4902
62	27.8395	0.6762	87.7132	31.4949	0.7840	87.8104
63	32.7779	0.6040	89.1044	32.8062	0.7037	89.0267
64	30.0384	0.4959	89.4961	28.2760	0.5690	89.3516
65	35.2053	0.6229	89.9332	37.2438	0.6923	89.9219
66	33.0220	0.6067	85.9995	29.3821	0.7037	86.0447
67	37.4149	0.7182	89.7655	35.9041	0.7846	89.9283
68	27.8741	0.5163	94.3705	33.6979	0.5811	94.3121
69	24.4510	0.5280	94.1530	24.3741	0.5995	94.1787
70	16.9879	0.6477	96.6457	22.4655	0.7017	96.6786
TOT	1640.091	36.5952	5444.704	1661.350	43.6266	5445.302
AVG	26.88671	0.590245	89.25745	27.23526	0.715190	89.26726
STD	4.886176	0.130548	4.232566	4.730469	0.122615	4.222276

21 - 25, and 27 all show a decrease for the visible reflectance. The scatter plots graphically show the great deal of variability in both the ship track and control group values. For example, Figure 16 shows a range in channel 1 ambient reflectance of 12 - 32% and in channel 3 ambient radiance of 0.5 - 0.75 $mWm^{-2}sr^{-1}cm$. Figure 16 shows a range in channel 1 ship track reflectance of 19 - 31% and in channel 3 ship track reflectance of 0.71 - 0.94 $mWm^{-2}sr^{-1}cm$. Coakley et al., attributed this variability to the irregularity in the distribution and size of cloud droplets within the same cloud mass, which serves to obscure some of the increase in channel 1 reflectivity. It is also shown in Figures 14 through 35, that the channel 3 near-infrared radiance values are higher in every case represented in this study, confirming similar observations made by Coakley et al.

Table 4 shows the small variability of the channel 4 radiance and also the almost negligible variation between ship track and control group radiance levels. Coakley et al., attributed this to the observation that at the channel 4 wavelength, liquid water is a strong absorber, therefore the amount of scattering is negligibly small. Also, there are enough droplets so that marine stratocumulus emit like black bodies regardless of droplet size and concentrations. Thus, there is no change in thermal emission between contaminated and noncontaminated clouds.

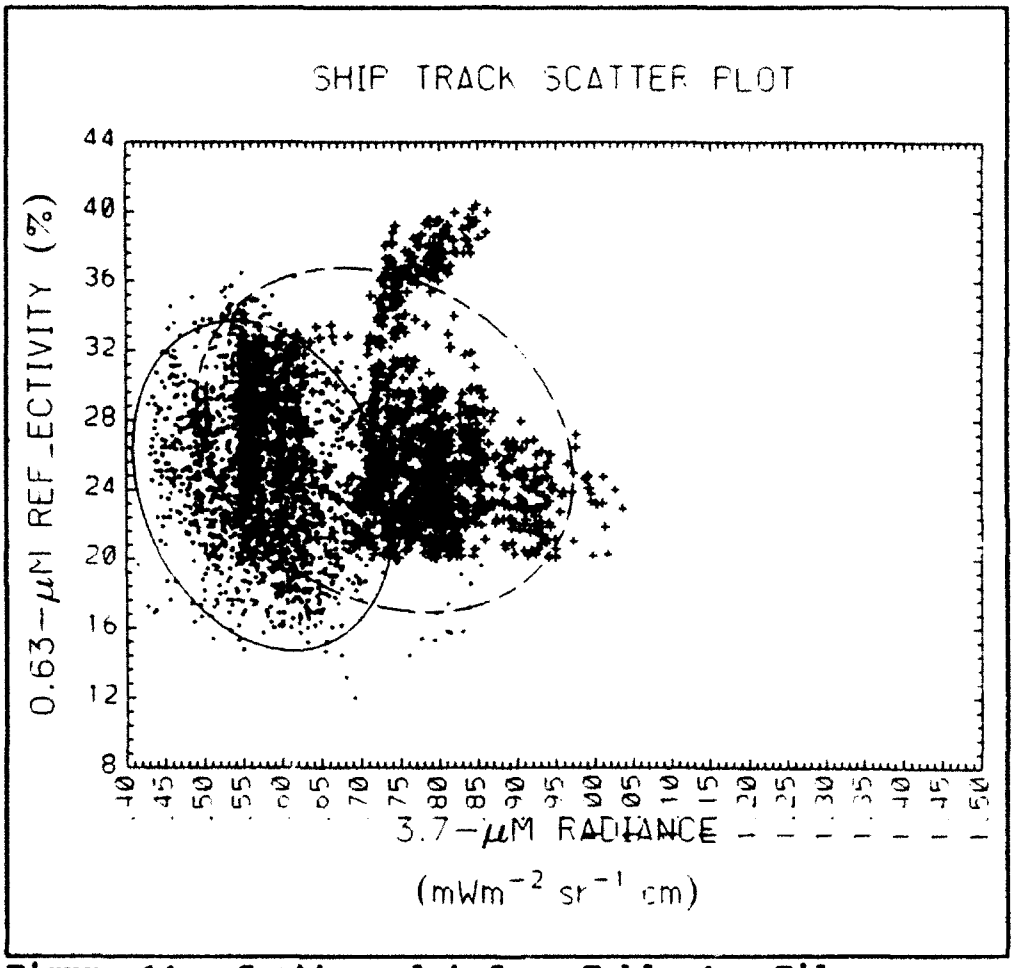

Figure 14. Scatter plot from Table 4 - File number 8. AR6105 (2314 UTC, 13/7/87).

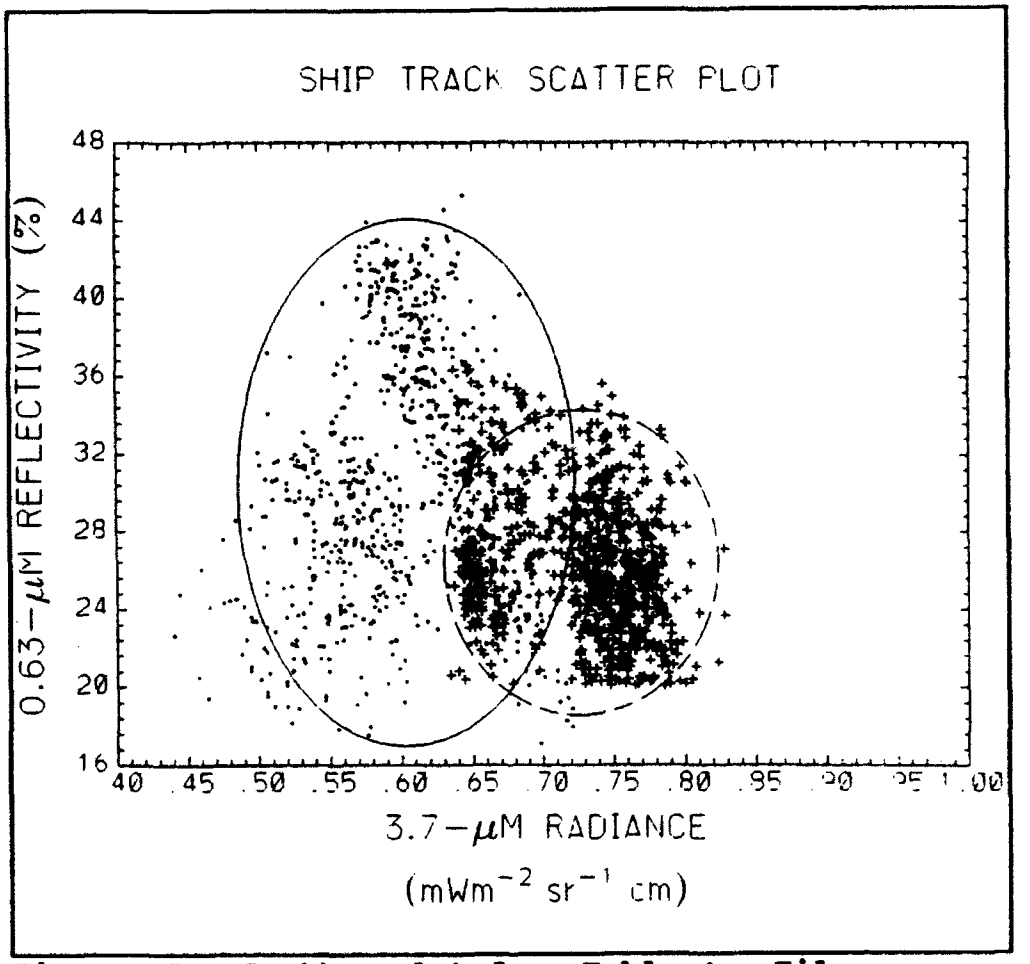

Figure 15. Scatter plot from Table 4 - File number 9. AR6105 (2314 UTC, 13/7/87).

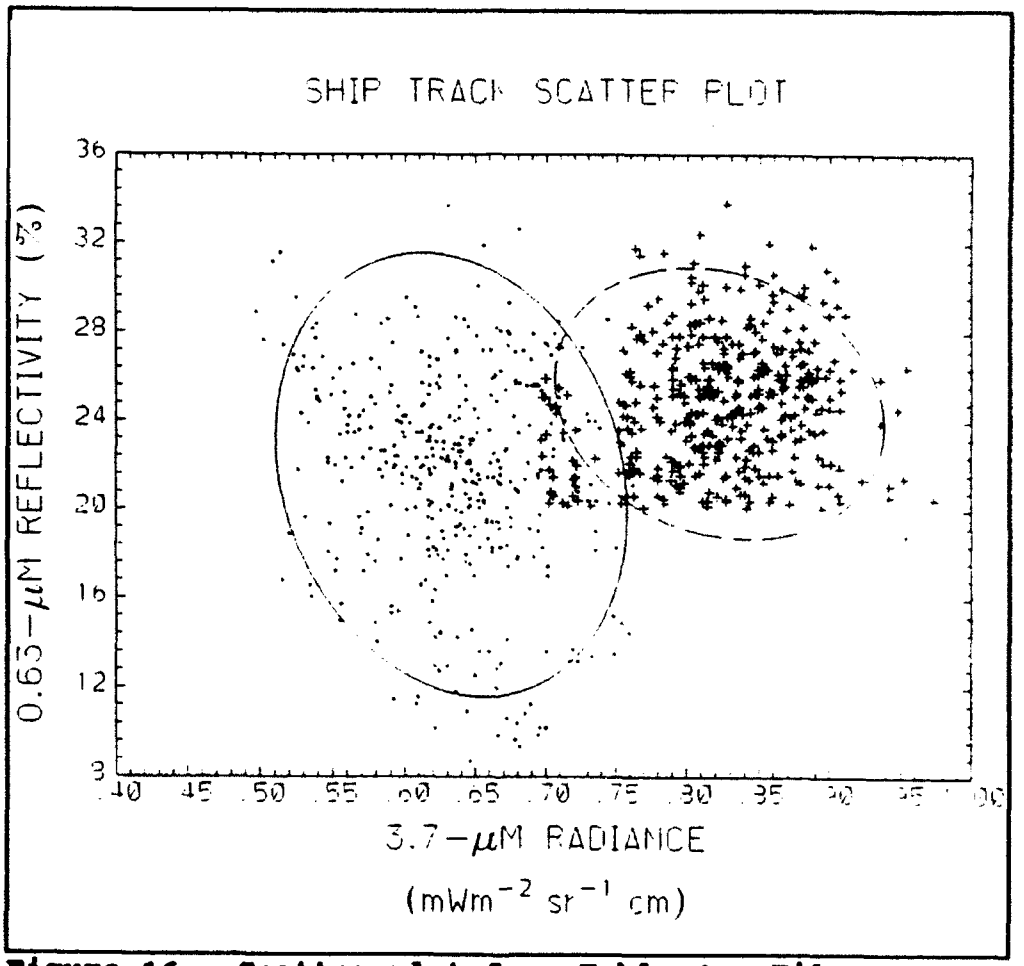

Figure 16. Scatter plot from Table 4 - File number 10. AR6105 (2314 UTC, 13/7/87).

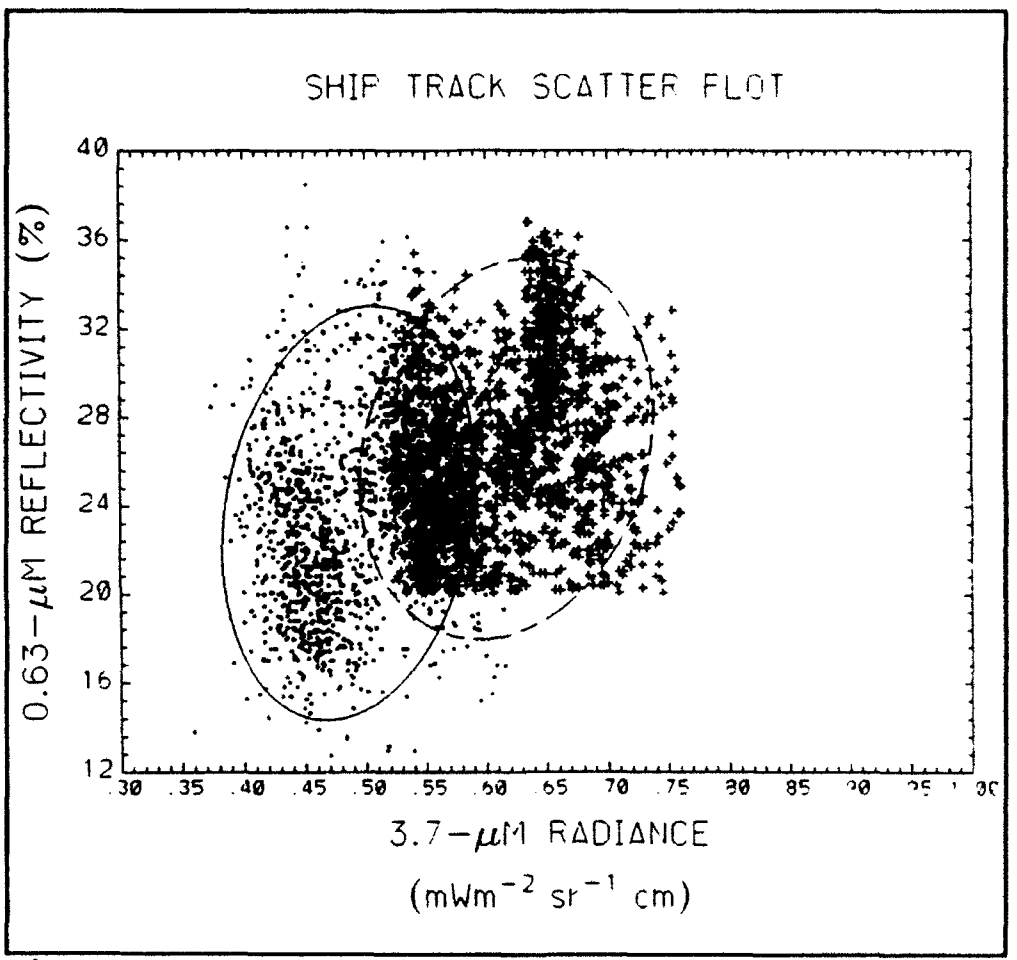

Figure 17. Scatter plot from Table 4 - File number 11. AR6105 (2314 UTC, 13/7/87).

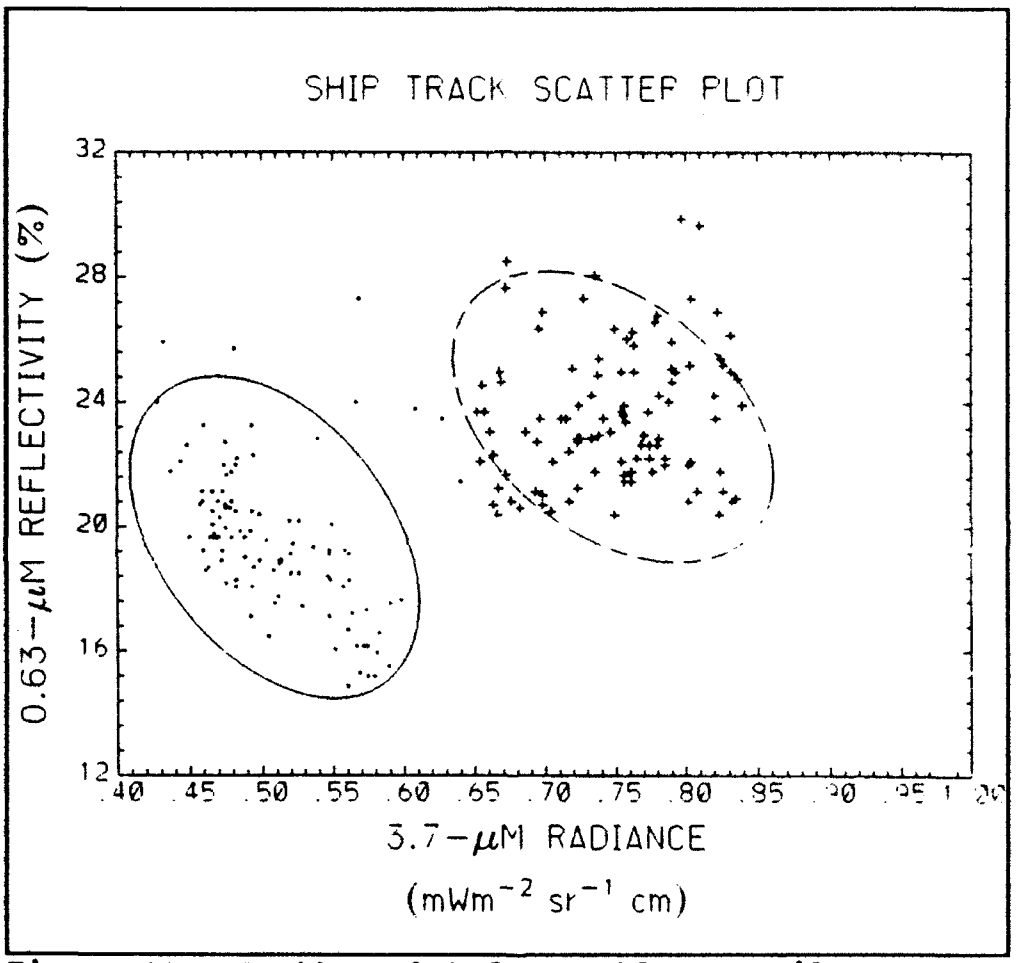

Figure 18. Scatter plot from Table 4 - File number 12. AR6105 (2314 UTC, 13/7/87).

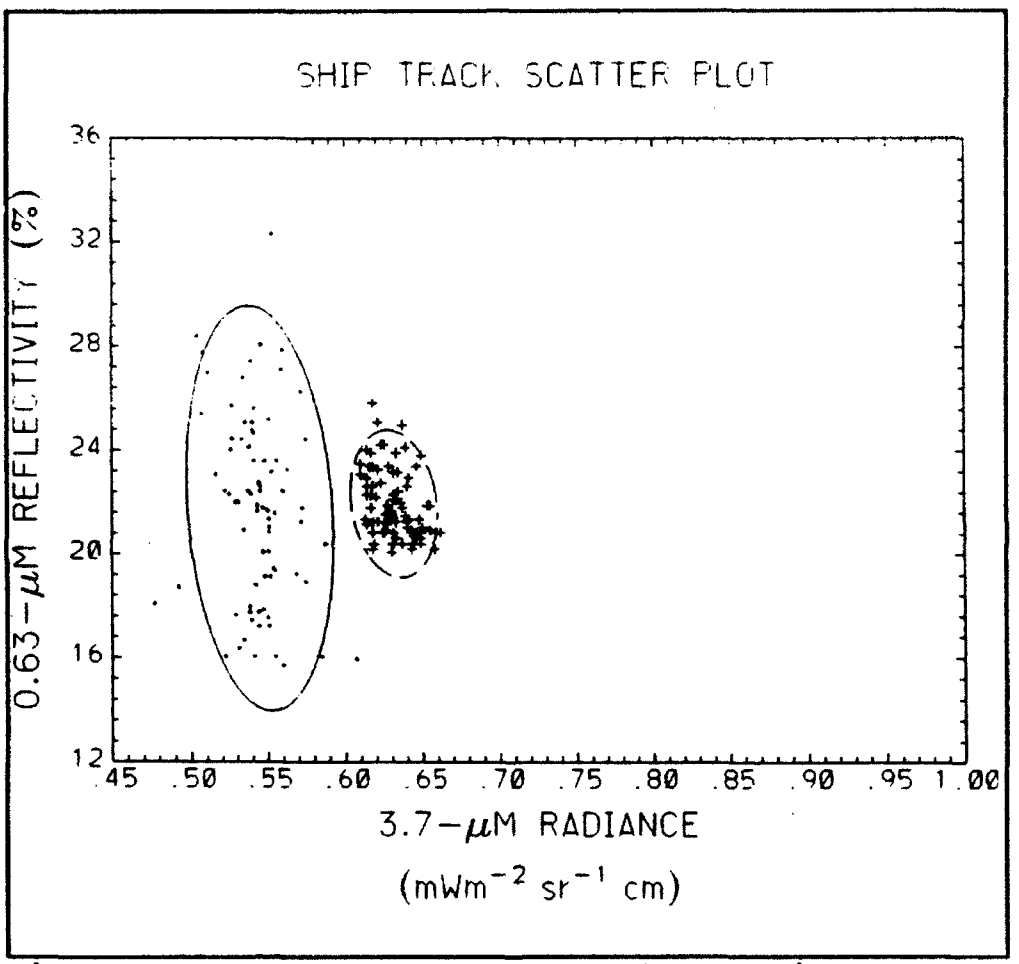

Figure 19. Scatter plot from Table 4 - File number 13. AR6105 (2314 UTC, 13/7/87).

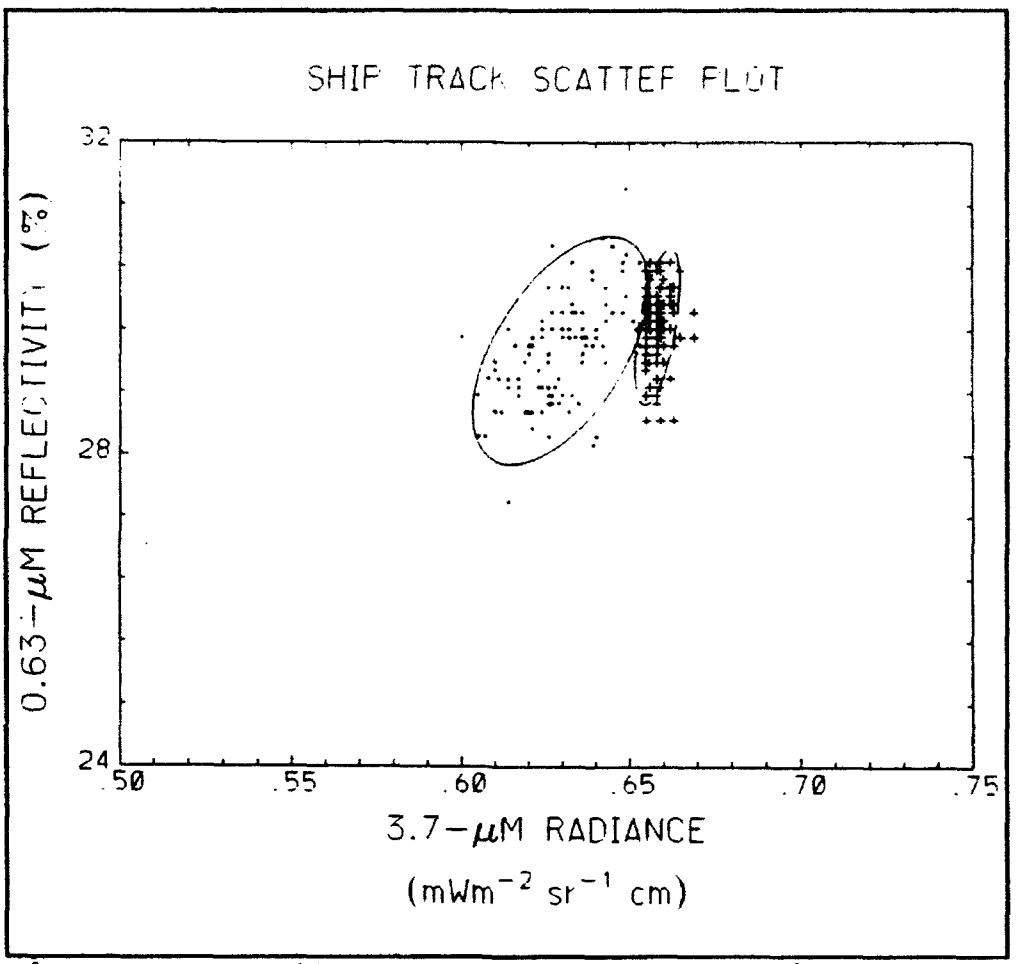

Figure 20. Scatter plot from Table 4 - File number 14. AR6113 (1526 UTC, 15/7/87).

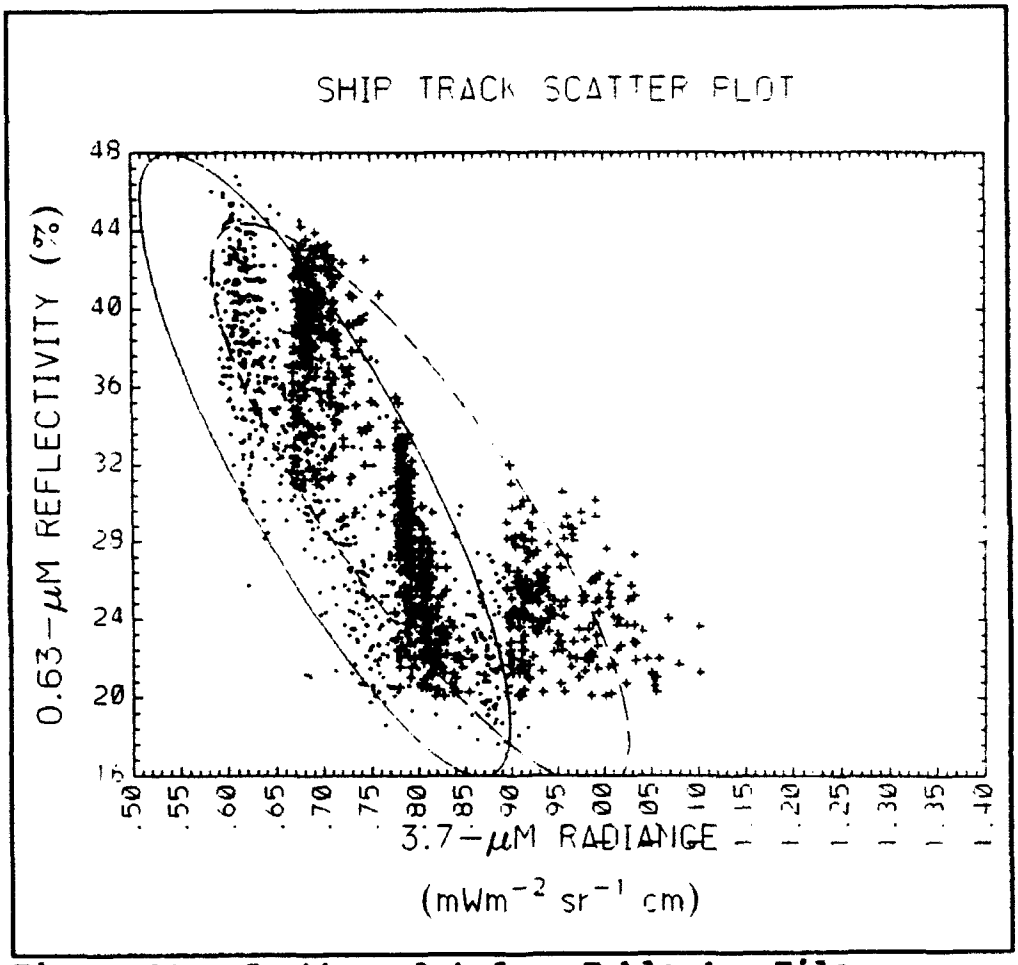

Figure 21. Scatter plot from Table 4 - File number 15. AR6114 (2252 UTC, 15/7/87).

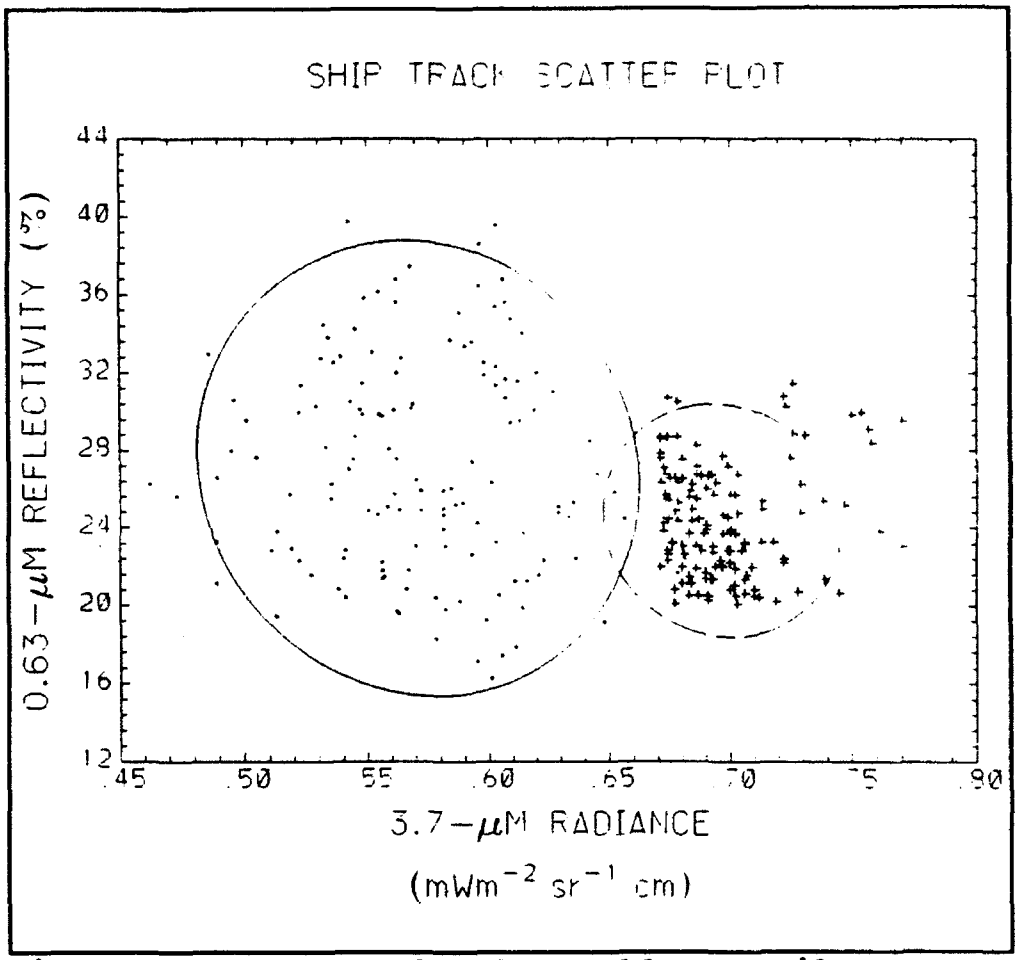

Figure 22. Scatter plot from Table 4 - File number 16. AR6114 (2252 UTC, 15/7/87).

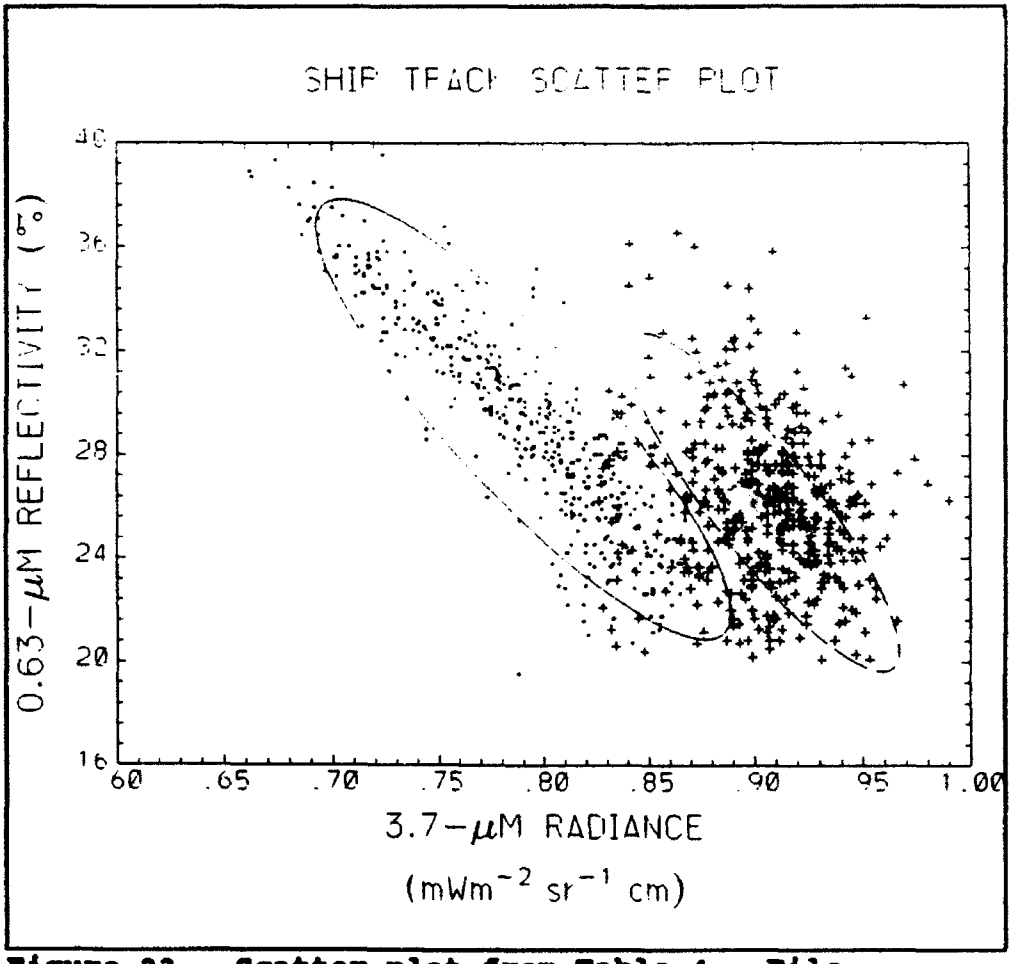

Figure 23. Scatter plot from Table 4 - File number 17. AR6114 (2252 UTC, 15/7/87).

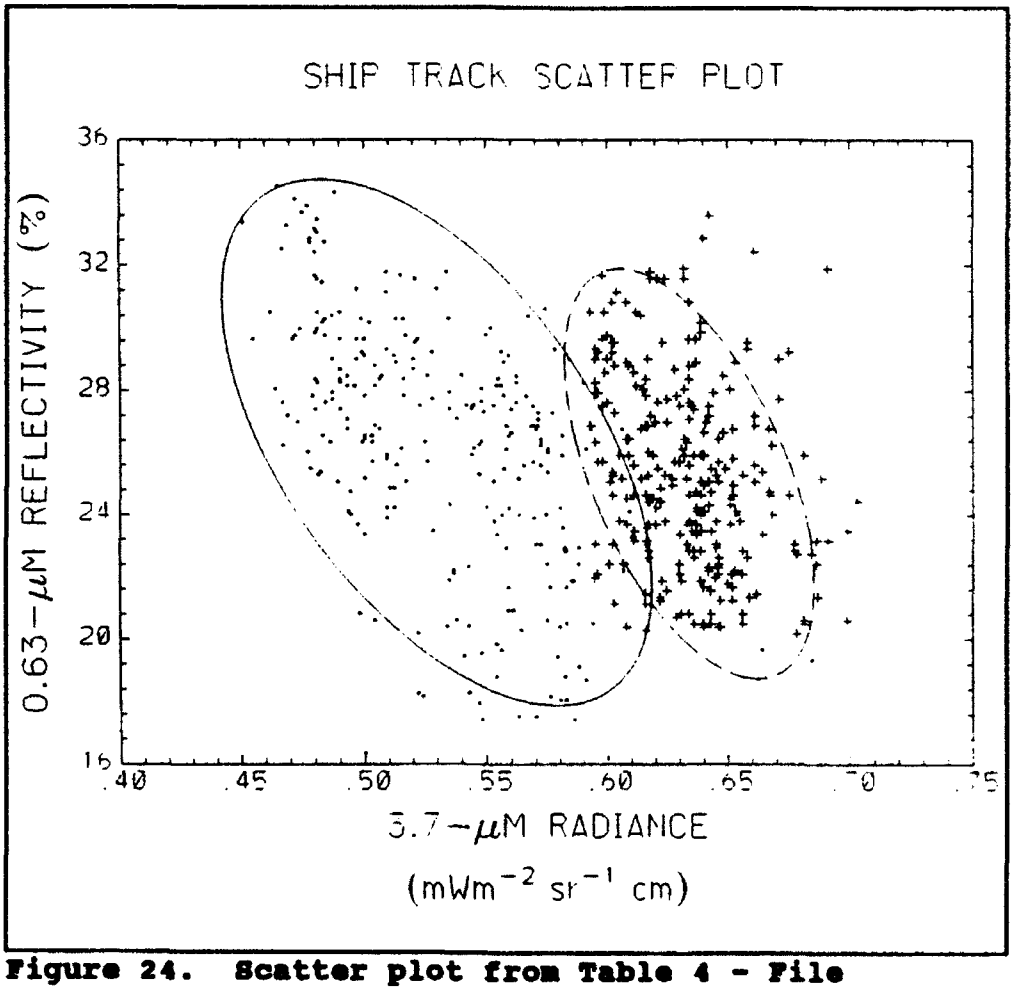

Figure 24. Scatter plot from Table 4 - File number 18. AR6120 (2231 UTC, 17/7/87).

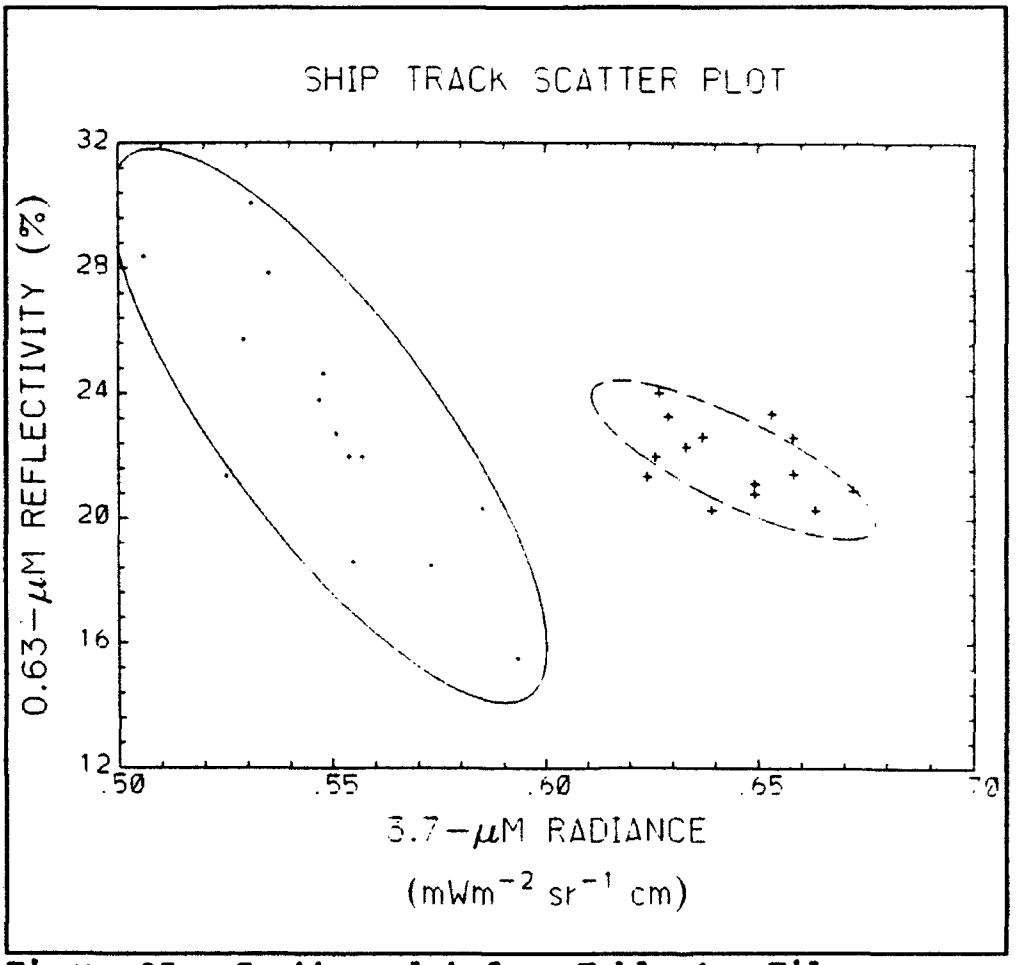

Figure 25. Scatter plot from Table 4 - File number 19. AR6120 (2231 UTC, 17/7/87).

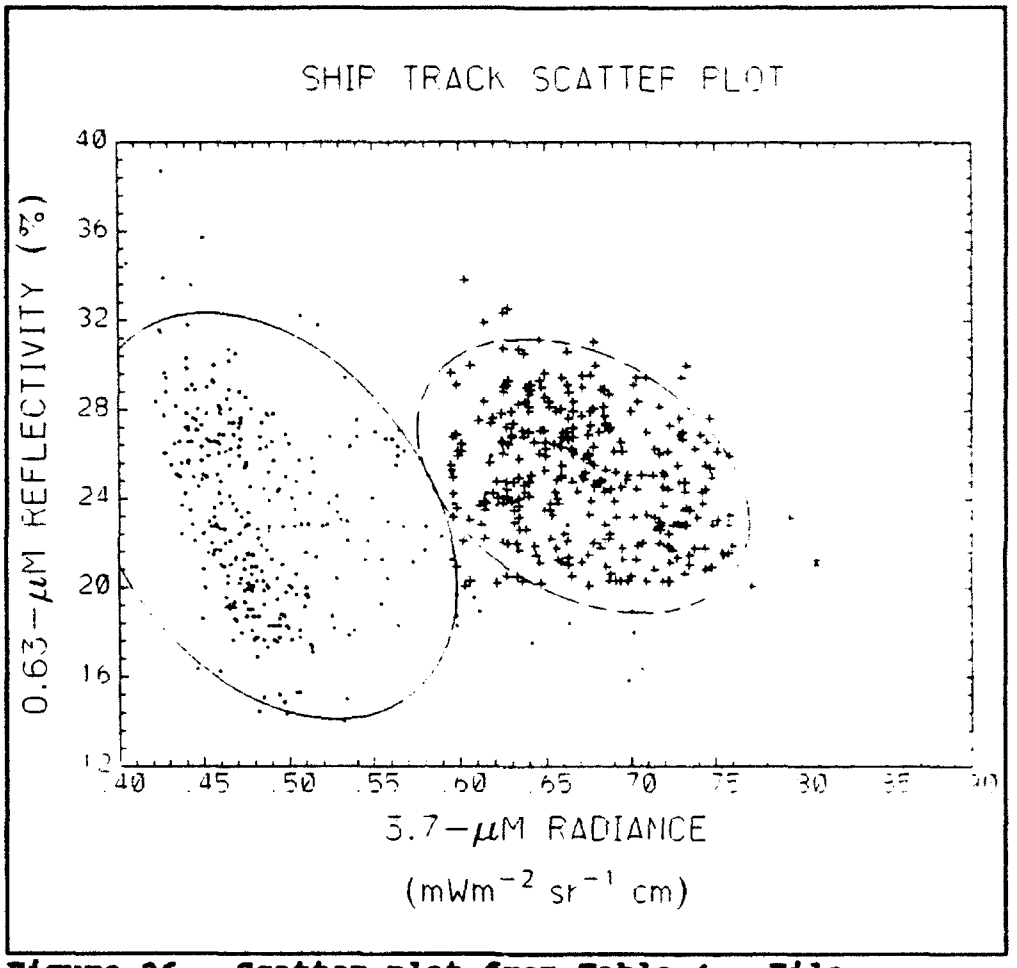

Figure 26. Scatter plot from Table 4 - File number 20. AR6049 (1529 UTC, 1/7/87).

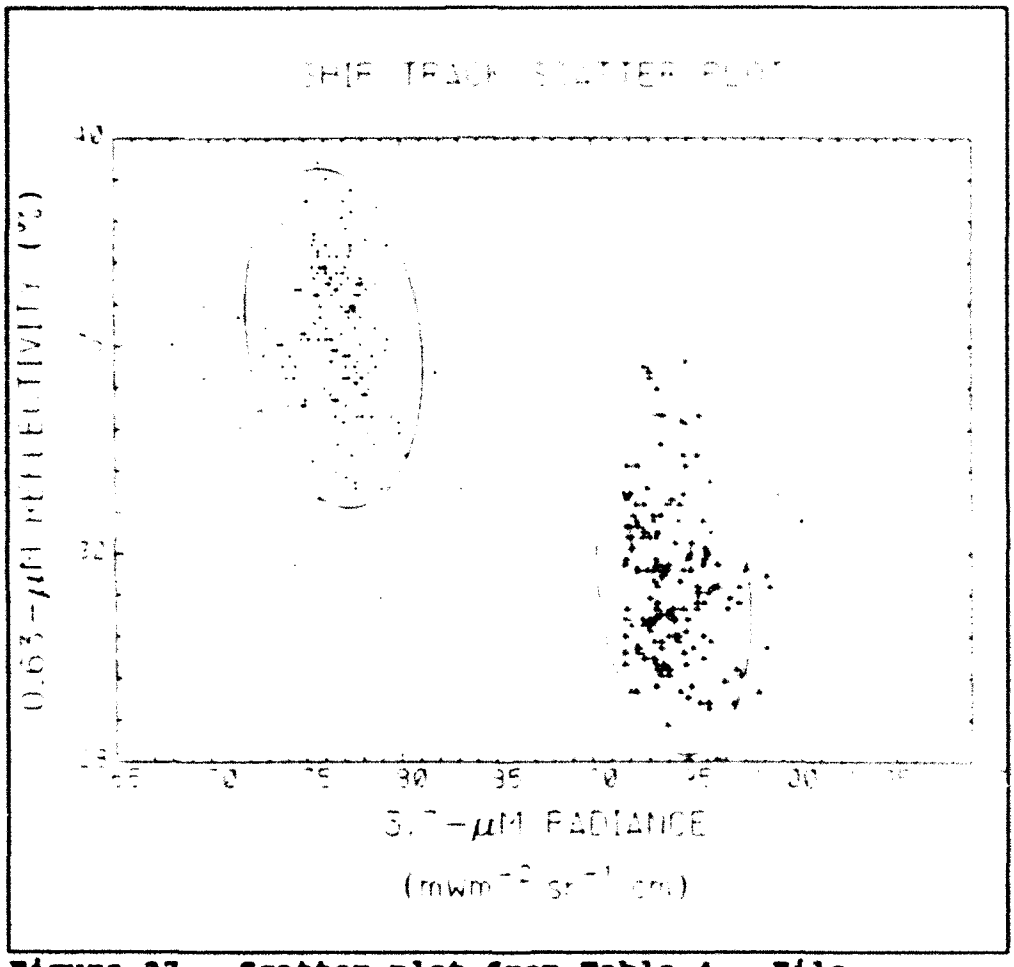

Figure 27. Scatter plot from Table 4 - File number 21. AR6049 (1529 UTC, 1/7/87).

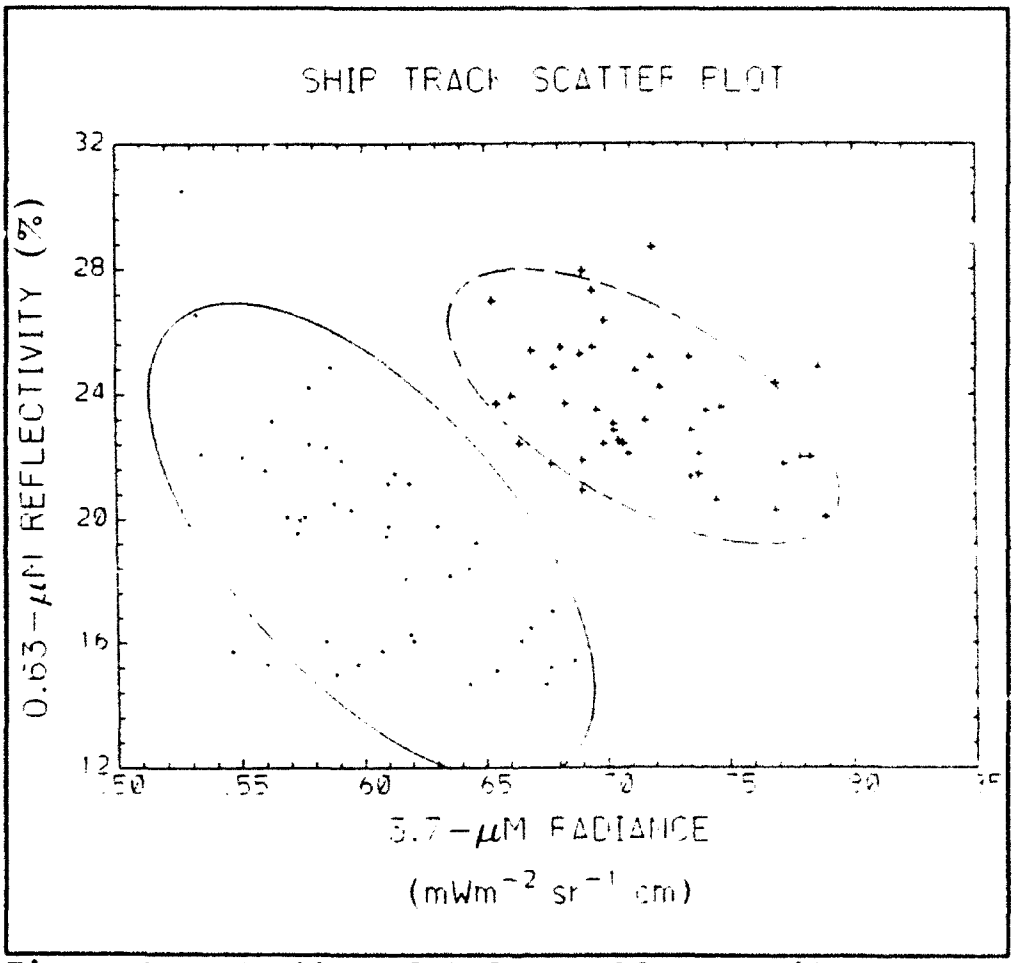

Figure 28. Scatter plot from Table 4 - File number 22. AR6049 (1529 UTC, 1/7/87).

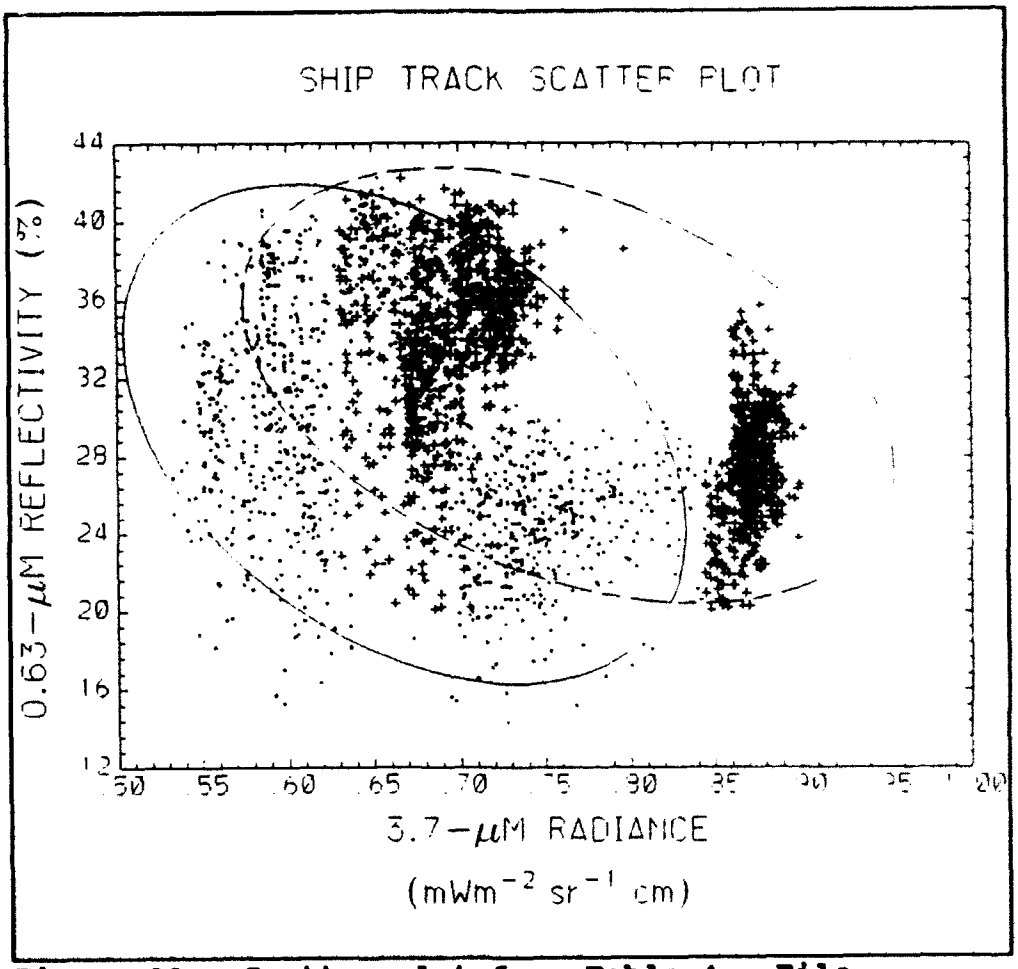

Figure 29. Scatter plot from Table 4 - File number 23. AR6049 (1529 UTC, 1/7/87).

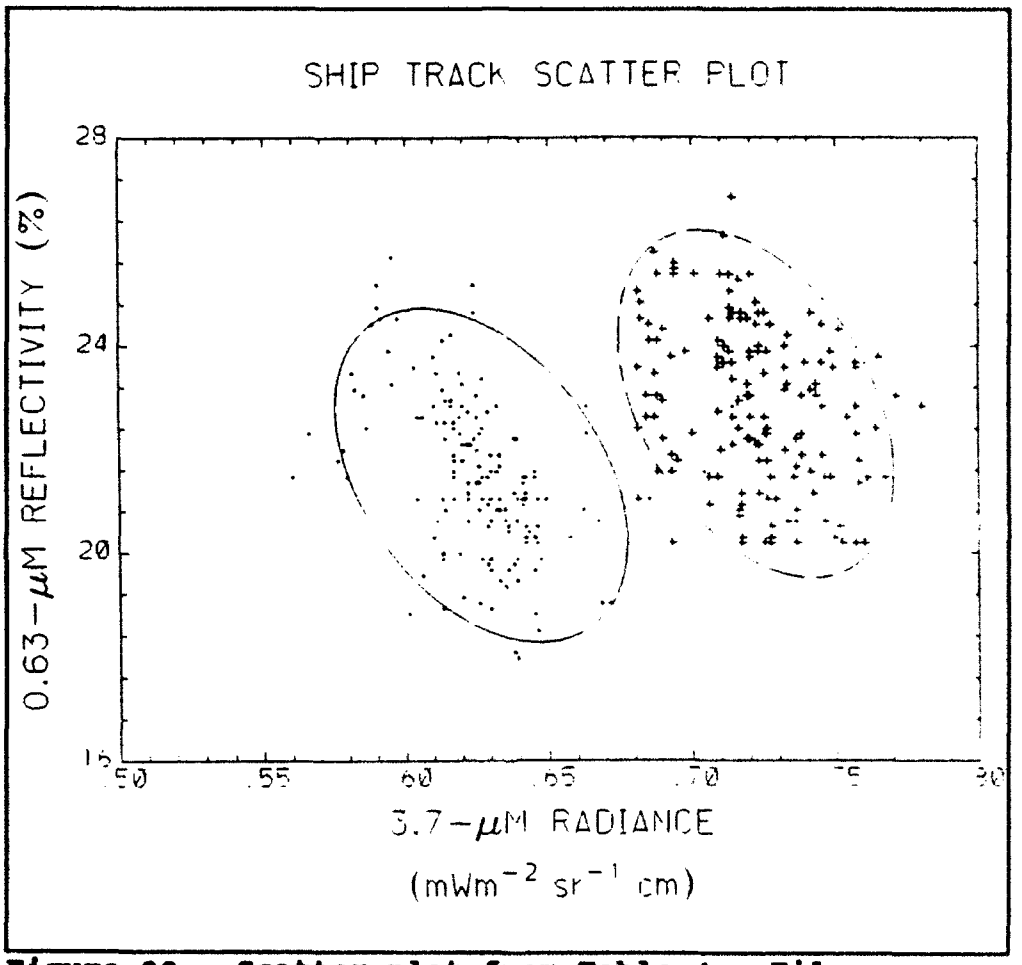

Figure 30. Scatter plot from Table 4 - File number 24. AR6049 (1529 UTC, 1/7/87).

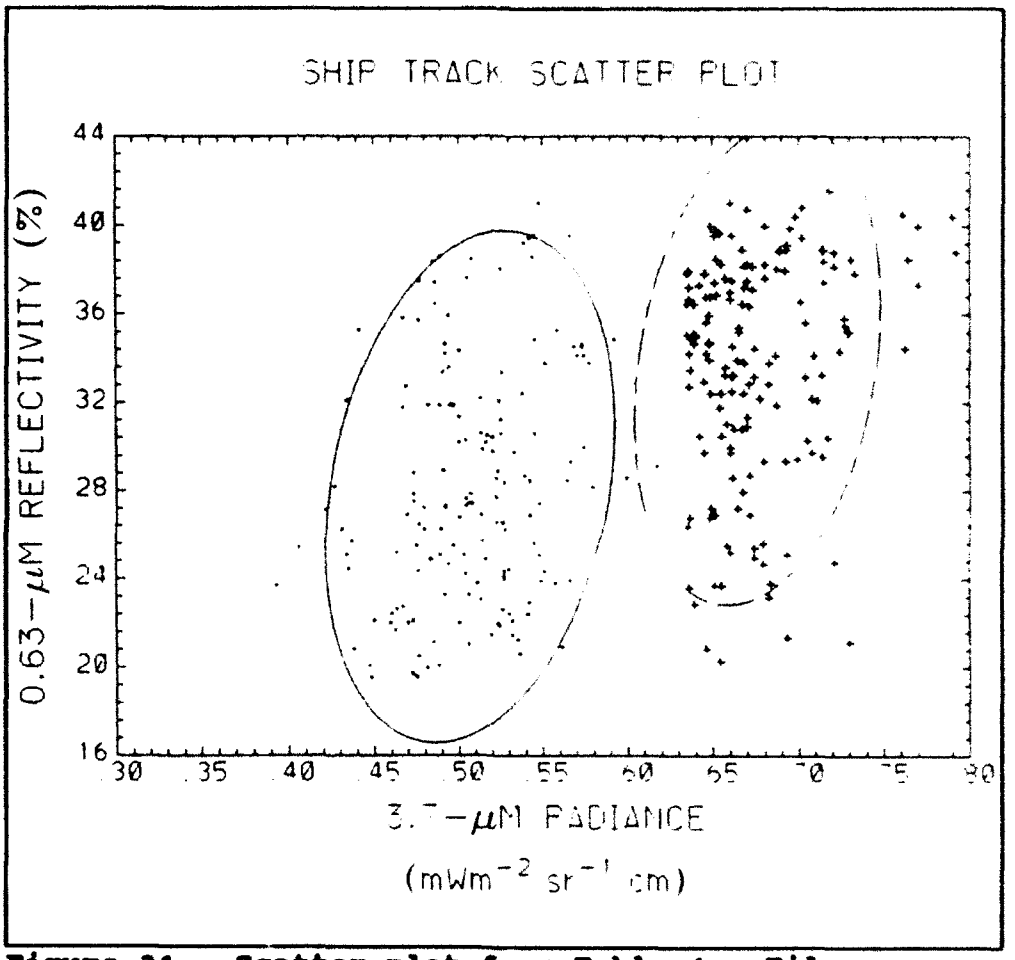

Figure 31. Scatter plot from Table 4 - File number 25. AR6051 (2213 UTC, 1/7/87).

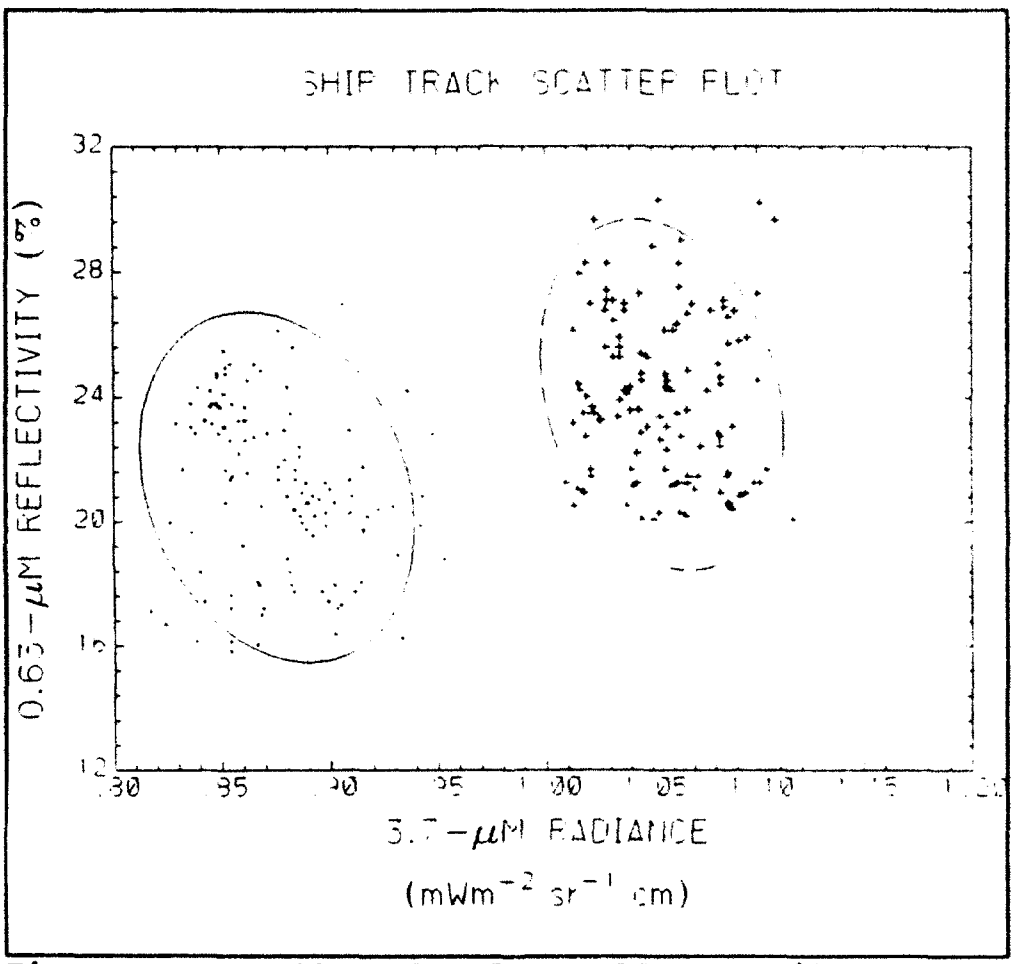

Figure 32. Scatter plot from Table 4 - File number 26. AR6051 (2213 UTC, 1/7/87).

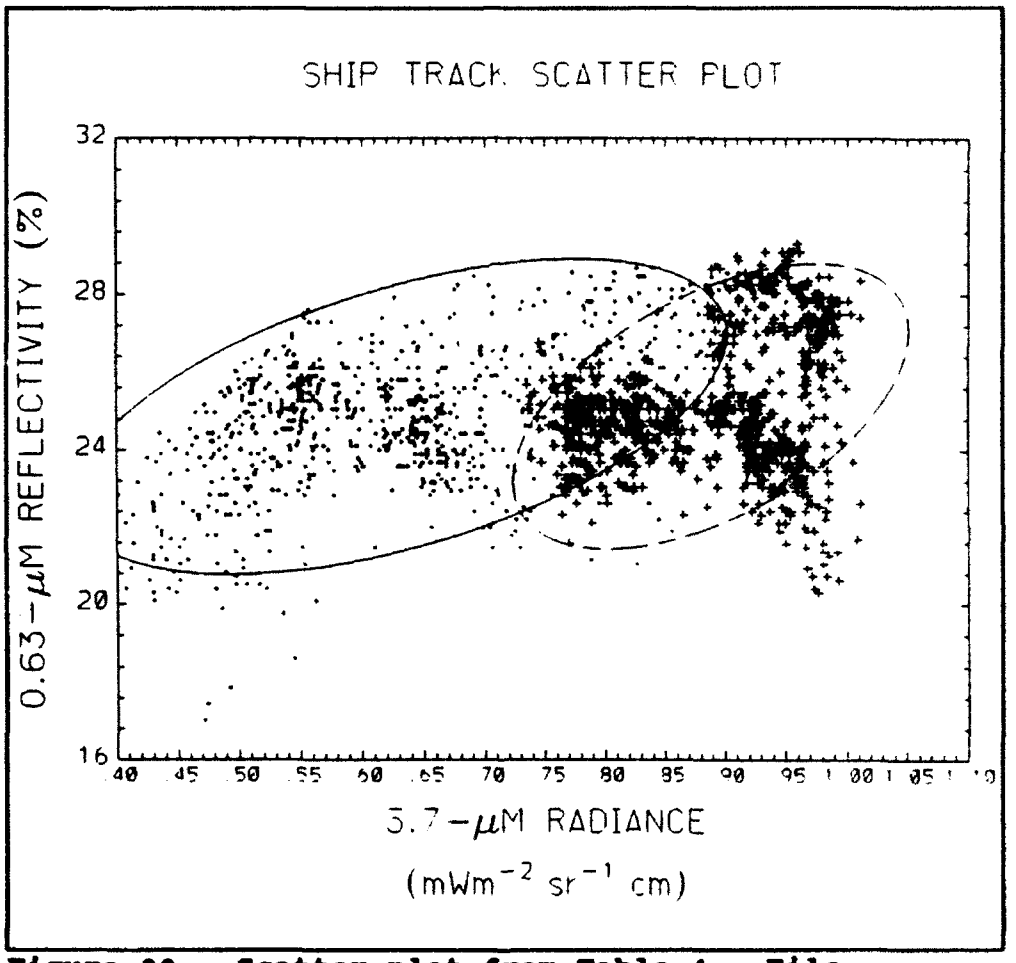

Figure 33. Scatter plot from Table 4 - File number 27. AR6054 (1508 UTC, 2/7/87).

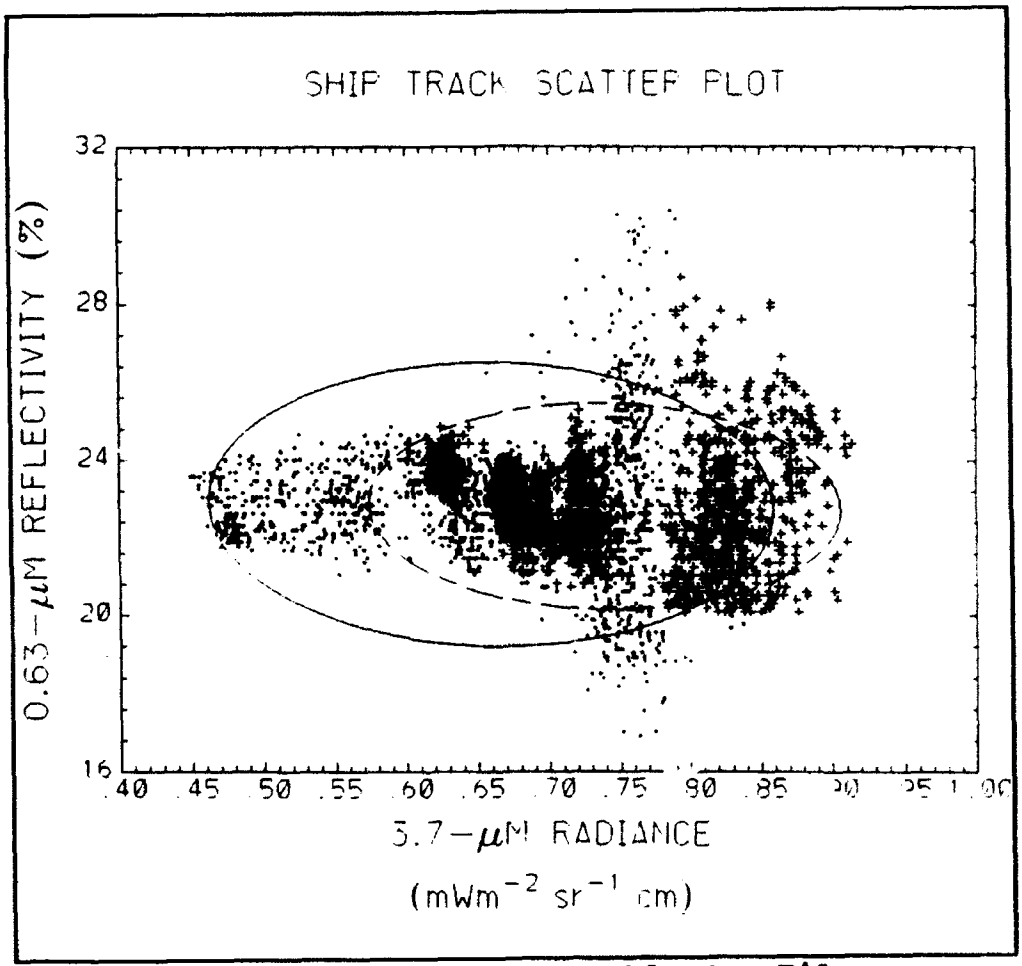

Figure 34. Scatter plot from Table 4 - File number 28. AR6054 (1508 UTC, 2/7/87).

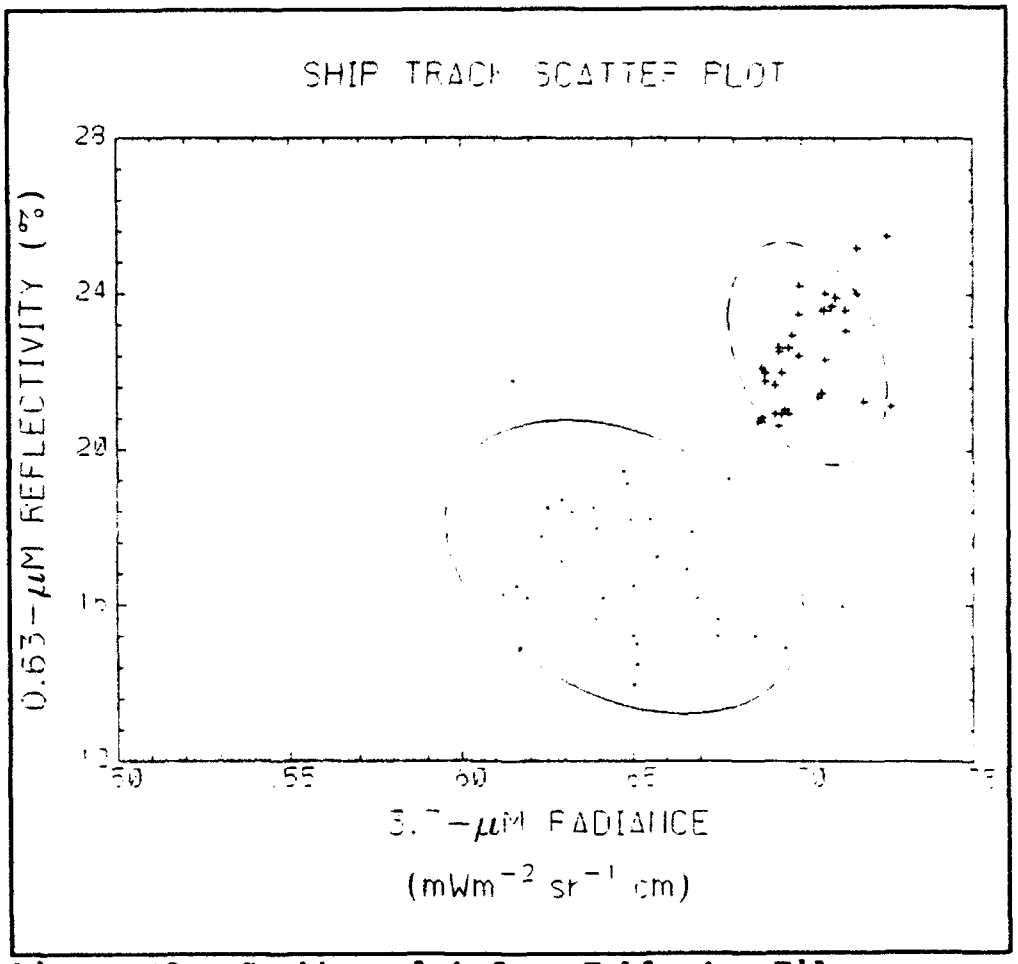

Figure 35. Scatter plot from Table 4 - File number 70. AR6113 (1526 UTC, 15/7/87).

Table 5 displays the differences in the ship track pixel means from the ambient pixel means. Table 5 also shows the conversion of channel 3 radiance to reflectivity. Table 5 shows that there is a marked increase in values for channels 1 and 3 in the ship track pixels compared to ambient pixels. Channel 1 ship track differences increased by 1.3% compared to ambient pixel means. Channel 3 ship track differences increased by 18.6% compared to the ambient pixels. One can also see that there is only a very slight increase in channel 4. This is again in support of the findings of Coakley et al. The percentage of increase in the values of reflectivity and radiance was found to be less in this study than that found in the results from Coakley et al., as seen in Table 6. Coakley et al., assumed that comparing the ratio of change in reflectivity for channel 1 to that for channel 3, removed the effect of fractional cloud cover which could influence the changes in the reflectivities noted above. The ratio of change in reflectivity for this analysis was 0.18 +/-1.4 which is nearly half the value of 0.4 +/- 0.8 found by Coakley et al.

TABLE 5

FILE	DIFFERENCES			CHANNEL 1
	CHN 1	CHN 3	CHN 4	REFLECTIVITY
8	2.6215	0.1566	-0.0712	3.070588
9	-4.1030	0.1225	0.1607	2.401960
10	3.2503	0.1879	0.1688	3.684313
11	2.8786	0.1297	-0.0524	2.541137
12	3.8698	0.2380	-0.1486	4.666666
13	0.1742	0.0865	0.0199	1.703921
14	0.3054	0.0289	-0.0948	0.566666
15	-2.1080	0.1017	0.2893	1.994117
16	-2.6661	0.1248	-0.0268	2.447058
17	-3.1728	0.1127	0.4324	2.209803
18	-0.9995	0.1033	-0.2754	2.025490
19	-1.0633	0.0949	0.0344	1.860784
20	1.7838	0.1828	0.1278	3.584313
21	1.2435	0.1773	0.2551	3.476470
22	4.1228	0.1112	-0.0271	2.180392
23	2.4715	0.0960	0.0390	1.882352
24	1.3610	0.0960	0.0077	1.882352
25	5.5805	0.1692	-0.1372	3.317647
26	2.9381	0.1790	0.0074	3.509803
27	0.2713	0.2542	-0.0396	4.984313
28	-0.0524	0.0793	0.0246	1.554901
29	5.5580	0.0961	0.0012	1.884313
30	-4.2801	0.1021	0.0193	2.001960
31	-2.1362	0.0890	-0.0512	1.745098
32	-4.0845	0.1213	0.0427	2.378431
33	-1.8324	0.2213	0.0880	4.339215
34	0.0293	0.1057	-0.0315	2.072549
35	-0.1661	0.1013	-0.0225	1.986274
37	-0.3547	0.0777	0.2046	1.523529
39	2.6337	0.1088	-0.0212	2.133333
40	0.1591	0.1079	-0.0303	2.115686
41	1.3145	0.2189	0.0921	4.292156
42	1.5940	0.0909	0.0141	1.782352
43	0.1300	0.0709	-0.0338	1.390196
44	0.2301	0.1041	-0.0036	2.041176
45	0.3007	0.1192	0.0529	2.337254
46	-2.8271	0.0789	0.0856	1.547058
47	-0.7039	0.1213	-0.2756	2.378431
48	0.4077	0.0725	-0.0211	1.421568
49	1.6916	0.0868	-0.0698	1.701960
50	-2.1637	0.1083	0.0957	2.123529
51	-2.6296	0.1312	-0.0629	2.572549
52	-3.5486	0.1104	-0.0325	2.164705
53	0.4450	0.0848	-0.1041	1.662745
54	0.3802	0.0590	0.0966	1.156862
55	0.4791	0.1034	0.0244	2.027450
56	0.4592	0.1456	0.0592	2.854901
57	0.2871	0.0570	-0.0209	1.117647
58	1.5921	0.1558	0.0243	3.054901
59	-2.1791	0.1008	-0.0227	1.976470
60	4.1413	0.1448	-0.0786	2.839215
61	3.4554	0.1990	-0.0061	3.901960
62	3.6554	0.1078	0.0972	2.113725
63	0.0283	0.0997	-0.0777	1.954901
64	-1.7624	0.0731	-0.1445	1.433333
65	2.0385	0.0694	-0.0113	1.360784
66	-3.6399	0.0970	0.0452	1.901960
67	-1.5108	0.0664	0.1628	1.301960
68	5.8218	0.0648	-0.0384	1.270588
69	-0.0769	0.0715	0.0257	1.401960
70	5.4776	0.0540	0.0329	1.058823
TOT	21.2599	7.0314	0.5982	117.8705
AVG	0.117458	0.111609	0.009495	2.188422
STD	2.596901	0.050292	0.120116	0.986134

TABLE 6 COMPARISON TO COAKLEY et al. (1987)			
CHANGE IN RADIANCE (mWm^{-2}-sr^{-1}-cm)	% REFLECTIVITY INCREASE		RATIO OF CHANGE IN REFLECTIVITY
CHANNEL 4	CHANNEL 1	CHANNEL 3	CHN1 / CHN3
COAKLEY et al. (1987)			
0.0+/-0.05	1.6+/-0.7	3.9+/-0.4	0.4+/-0.8
LUTZ			
0.0+/-0.12	0.34+/-2.6	2.1+/-0.99	0.16+/-2.6

IV. CONCLUSIONS AND RECOMMENDATIONS

The primary focus of this thesis involved evaluating a large satellite data set to determine the number and geographical position of ship tracks that occurred during the period of study (1 - 19 July 1987). In total, 316 ship tracks were located and plotted. A statistical evaluation was then conducted on the radiative properties of the confirmed ship tracks.

It was discovered that 22 of the 28 (76%) satellite passes evaluated in this thesis contained ship tracks. The 76% was shown to be significantly higher than the 5 to 10% expected in the earlier by Coakley et al. (1987). It was shown that the AVHRR channel 3 was more favorable to the observance of ship tracks than channel 1.

The large number of ship tracks found, provided a rich data set which was evaluated using the modified Coakley algorithm for automatic ship track detection. The statistical study concurred with the conclusions of Coakley et al., that ship exhaust increases the reflective properties of clouds. Table 4 indicated there is substantial variability of the cloud radiative properties, which show up clearly when examining the ship track and ambient pixels for channels 1, 3 and 4. When considering the means, all three channels showed an increase in the ship pixels compared to the

ambient pixels. The increase for channels 1 and 3 was significant (0.35 +/- 2.6% reflectivity for channel 1 and 0.11 +/- 0.05 $mWm^{-2}sr^{-1}cm$ for channel 3) and very slight for channel 4 (0.01 +/- 0.12 $mWm^{-2}sr^{-1}cm$). Although all three channels showed increases in radiative properties, as in Coakley et al., the increases were less for this study.

Many areas of research have yet to be explored in the study of ship tracks. Some of the areas for future work are:

1. Investigation of weather patterns within areas of known ship track formation should be conducted to determine more precisely what factors encourage the formation of ship tracks.
2. An effort should be made to discover the cause of the variability found in the reflectivity and radiance readings associated with the ship track.
3. Work should be continued to improve the ability of the Coakley algorithm to process satellite data and automatically locate and analyze ship tracks. Additionally the algorithm should be developed to automatically create a plot of ship tracks found.
4. Studies are still needed to determine if specific ship types can be associated with variations in ship track properties.

The study of ship track formation will be a continuing source of exciting research in the years to come. Civilian and military use of the ability to monitor the movements of ships by evaluating their ship tracks is very promising. With the growing worldwide concern about our environment, the efforts expended on ship track formation processes will pay great dividends in our efforts to protect our fragile planet.

LIST OF REFERENCES

Albrecht, B. A., 1989: Aerosols, cloud microphysics and fractional cloudiness. *Science*, **245**, 1227-1230.

Allen, R. C., Jr., 1987: Automated satellite cloud analysis: A multispectral approach to the problem of snow/cloud discrimination. M.S. thesis, Naval Postgraduate School, Monterey, CA, May 1987, 66 pp.

Coakley, J. A., Jr., R. L. Bernstein and P. A. Durkee, 1987: Effect of ship stack effluents on cloud reflectivity. *Science*, **237**, 953-1084.

Conover, J. H., 1969: New observations of anomalous cloud lines. *J. Atmos. Sci.*, **24**, 1153-1154.

Fett, R. W., P. E. La Violette, M. Nestor, J. W. Nickerson and R. Rabe, (1979): Navy tactical applications guide. volume II, environmental phenomena and effects. Department of the Navy, Washington, D. C., NEPRF Technical Report 77-04, 161 pp.

Hindman, E. E., II, P. V. Hobbs and L. F. Radke, 1977: Cloud condensation nucleus size distributions and their effects on cloud droplet size distributions. *J. Atmos. Sci.*, **34**, 951-956.

Hunt, G. E., 1972: Radiative properties of terrestrial clouds at visible and infra-red thermal window wavelengths. *Quart. J. R. Met. Soc.*, **99**, 346-369.

Morehead, S. E., 1988: Ship track cloud analysis for the North Pacific area. M.S. thesis, Naval Postgraduate School, Monterey, CA, September 1988, 57 pp.

Twomey, S., 1977: The influence of pollution on the shortwave albedo of clouds. *J. Atmos. Sci.*, **34**, 1149-1152.

Twomey, S. and T. Cocks, 1982: Spectral reflectance of clouds in the near-infrared: comparison of measurements and calculations. *J. Meteor. Soc. Japan*, **60**, 583-592.

Twomey, S., H. B. Howell and T. A. Wojciechowski, 1968: Comments on "anomalous cloud lines". *J. Atmos. Sci.*, **25**, 333-334.

Twomey, S., M. Piepgrass and T. L. Wolfe, 1984: An assessment of the impact of pollution on global cloud albedo. *Tellus*, **36B**, 356-366.

INITIAL DISTRIBUTION LIST

		No. Copies
1.	Defense Technical Information Center Cameron Station Alexandria, VA 22304-6145	2
2.	Library, Code 52 Naval Postgraduate School Monterey, CA 93943-5000	2
3.	Chairman (Code OC/Co) Department of Oceanography Naval Postgraduate School Monterey, CA 93943-5000	1
4.	Chairman (Code MR/Hy) Department of Meteorology Naval Postgraduate School Monterey, CA 93940-5000	1
5.	Professor Philip A. Durkee Department of Meteorology Naval Postgraduate School Monterey, CA 93940-5000	1
6.	Professor Carlyle H. Wash Department of Meteorology Naval Postgraduate School Monterey, CA 93940-5000	1
7.	Lt.Cdr. John W. Lutz 28 Revere Rd. Monterey, CA 93940	1
8.	Commander Naval Oceanography Command Stennis Space Center MS 39529-5000	1
9.	Commanding Officer Naval Oceanographic Office Stennis Space Center MS 39529-5001	1

10. Commanding Officer 1
Fleet Numerical Oceanography Center
Monterey, CA 93943-5005

11. Commanding Officer 1
Naval Research Laboratory
Stennis Space Center
MS 39529-5004

12. Superintendent 1
Naval Research Laboratory
NPS Annex, Code 7500
Monterey, CA 93943-5006

13. Chief of Naval Research 1
800 N. Quincy Street
Arlington, VA 22217